The Cryosphere Discuss., 8, 4681–4735, 2014
www.the-cryosphere-discuss.net/8/4681/2014/
doi:10.5194/tcd-8-4681-2014

The Cryosphere Discussions
Open Access

Area, volume and mass changes of southeast Vatnajökull ice cap, Iceland, from the Little Ice Age maximum in the late 19th century to 2010

H. Hannesdóttir, H. Björnsson, F. Pálsson, G. Aðalgeirsdóttir, and S. Guðmundsson

Institute of Earth Sciences, University of Iceland, 101 Reykjavík, Iceland

Received: 8 August 2014 – Accepted: 22 August 2014 – Published: 5 September 2014

Correspondence to: H. Hannesdóttir (hrafnha@hi.is)

Published by Copernicus Publications on behalf of the European Geosciences Union.

Abstract

Area and volume changes and the average geodetic mass balance of the non-surging outlet glaciers of southeast Vatnajökull ice cap, Iceland, during different time periods between ~ 1890 and 2010, are derived from a multi-temporal glacier inventory. A series of digital elevation models (DEMs) (~ 1890, 1904, 1936, 1945, 1989, 2002, 2010) have been compiled from glacial geomorphological features, historical photographs, maps, aerial images, DGPS measurements and a LiDAR survey. Given the mapped bedrock topography we estimate relative volume changes since the end of the Little Ice Age (LIA) ~ 1890. The variable dynamic response of the outlets, assumed to have experienced similar climate forcing, is related to their different hypsometry, bedrock topography, and the presence of proglacial lakes. In the post-LIA period the glacierized area decreased by 164 km^2 and the glaciers had lost 10–30 % of their ~ 1890 area by 2010. The glacier surface lowered by 150–270 m near the terminus and the outlet glaciers collectively lost 60 ± 8 km^3 of ice, which is equivalent to 0.154 ± 0.02 mm of sea level rise. The relative volume loss of individual glaciers was in the range of 15–50 %, corresponding to a geodetic mass balance between −0.70 and −0.32 m w.e. a^{-1}. The rate of mass loss was most negative in the period 2002–2010, on average -1.34 ± 0.12 m w.e. a^{-1}, which lists among the most negative mass balance values recorded worldwide in the early 21st century. From the data set of volume and area of the outlets, spanning the 120 years post-LIA period, we evaluate the parameters of a volume-area power law scaling relationship.

1 Introduction

Area changes and glacier retreat rates since the Little Ice Age (LIA) maximum are known from glacierized areas worldwide (e.g., Haeberli et al., 1989; WGMS, 2008). The majority of glaciers have been losing mass during the past century (Vaughan et al., 2013), and a few studies have estimated the volume loss and the mass balance for the post-LIA period by various methods (e.g., Rabatel et al., 2006; Bauder et al., 2007; Knoll et al., 2008; Lüthi et al., 2010; Glasser et al., 2011). Knowledge about the ice volume stored in glaciers at different times is important for past, current and future estimates of sea level rise. Ice caps and glaciers outside polar areas have contributed more than half of the land ice to the global mean sea level rise in the 20th century (Church et al., 2013). Furthermore, glacier inventories are important to analyze and assess glacier changes at a regional scale, and they provide a basic data set for glaciological studies, for example to calibrate models simulating future glacier reponse to changes in climate.

Iceland is located in a climatically variable area of the North Atlantic Ocean, influenced by changes in the atmospheric circulation and warm and cold ocean currents. The temperate maritime climate of Iceland is characterized by small seasonal variations in temperature, on average close to 0 °C in the winter and 11 °C during the summer months in the lowland. The temperate glaciers and ice caps receive high amounts of snowfall, induced by the cyclonic westerlies crossing the North Atlantic and have mass turnover rates in the range of 1.5–3.0 m w.e. a^{-1} (Björnsson et al., 2013). Simulations with a coupled positive-degree-day and ice flow model reveal that Vatnajökull is one of the most sensitive ice cap in the world, and the mass balance sensitivity of southern Vatnajökull is in the range of 0.8–1.3 m w.e. a^{-1} 1 °C^{-1} (Aðalgeirsdóttir et al., 2006); among the highest in the world (De Woul and Hock, 2005). Apart from Greenland, the highest rate of meltwater input to the North Atlantic Ocean, comes from the Icelandic glaciers, that have contributed ~ 0.03 mm a^{-1} on average to sea level rise since the mid-1990s (Björnsson et al., 2013). Only a few quantitative estimates on volume and mass balance changes of the entire post-LIA period are available for Icelandic glaciers (Flowers et al., 2007; Aðalgeirsdóttir et al., 2011; Pálsson et al., 2012; Guðmundsson, 2014).

The outlet glaciers of southeast Vatnajökull (Fig. 1) are located in the warmest and wettest area of Iceland and descend down to the lowlands. Results of spatially distributed coupled models of ice dynamics and hydrology, indicate that these glaciers are the most sensitive to future warming of all outlets of Vatnajökull (Flowers et al., 2005). They are particularly vulnerable to warming climate conditions, since their beds lie even 100–300 m below the elevation of the current terminus (Björnsson and Pálsson, 2008). The surface geometry of the outlet glaciers at the LIA maximum has been reconstructed from glacial geomorphological features and historical data (Hannesdóttir et al., 2014). The outlets were at their terminal LIA moraines around ~ 1890, which marked the termination of the LIA in Iceland (Thórarinsson, 1943; Hannesdóttir et al., 2014).

To estimate the downwasting, area and volume loss and geodetic mass balance of the outlets of southeast Vatnajökull since ~ 1890, glacier outlines have been digitized from various sources, and digital elevation models (DEMs) created from contour lines of topographic maps, DGPS measurements and various airborne surveys. The equilibrium line altitude (ELA) has been estimated from a series of recent MODIS images. We consider the different response of the glaciers to similar climate forcing during the post-LIA time period, and from the constructed record of area and volume changes, the scaling parameters of a power law which relates glacier area to volume are evaluated.

2 Study area and previous work

The studied outlet glaciers of southeast Vatnajökull are non-surging, less than 100 km apart and most of them reach down to 20–100 m a.s.l. (Fig. 1). The glaciers vary in size from 10–200 km^2, their average thickness range is 80–330 m (Table 1), and the hypsometry (area distribution with altitude) differs considerably. Morsárjökull, the westernmost outlet, flows down from an ice divide of ~ 1350 m. Öræfajökull (2100 m a.s.l.) feeds several outlet glaciers: the eastern part of Skaftafellsjökull, Svínafellsjökull, Kotárjökull, Kvíárjökull, Hrútárjökull and Fjallsjökull (Fig. 1). East of Breiðamerkurjökull, three outlet glaciers descend from the 1500 m high plateau of the Breiðabunga dome, Skálafellsjökull, Heinabergsjökull, and Fláajökull. Further east is Hoffellsjökull, and its accumulation area lies between Breiðabunga and the mountainous area of Goðahnúkar (1500 m), which feeds Lambatungnajökull (Fig. 1). The outlet glaciers east of Breiðamerkurjökull are hereafter referred to as the eastern outlet glaciers. The bedrock topography of the studied outlets is known from radio echo sounding measurements (Björnsson, 2009; Magnússon et al., 2012). The glaciers terminate in glacially eroded alpine-like valleys and have carved into soft glacial and glacio-fluvial sediments. It is unlikely that the troughs were only formed during the LIA, considering the present rate of sediment transport in the main glacial rivers of Öræfajökull (Magnússon et al., 2012). Many of them presently calve into proglacial lakes, which enhances ablation, and makes them vulnerable to predicted future warming (Björnsson and Pálsson, 2008; Magnússon et al., 2012).

Mass balance measurements have been carried out on Vatnajökull since 1993, and the ice cap has lost 1 m w.e. a^{-1} on average since (Björnsson et al., 2013). The majority of the survey stakes are located on the northern and western outlet glaciers (Fig. 1), but a number of stakes are situated on Breiðamerkurjökull and the eastern outlets (Björnsson and Pálsson, 2008; Aðalgeirsdóttir et al., 2011). In the accumulation area of these last-mentioned outlets, annual mass balance has been measured 1–4 m w.e. a^{-1} in the time period 1996–2010. Losses of up to 9 m w.e. a^{-1} have been observed during summer on Breiðamerkurjökull and Hoffellsjökull, and even negative winter balances at the terminus (Björnsson and Pálsson, 2008). The mass balance at the plateau of Öræfajökull ice cap was 6–8 m w.e. a^{-1} in 1993–1998 (Guðmundsson, 2000). Based on satellite imagery, in situ mass balance measurements and model simulations, the average ELA of southeast Vatnajökull has been estimated to be around 1100–1200 m (Björnsson, 1979; Aðalgeirsdóttir et al., 2005, 2006; Björnsson and Pálsson, 2008; Aðalgeirsdóttir et al., 2011). Interannual variability of the ELA has been measured approximately 200–300 m in the time period 1992–2007 (Björnsson and Pálsson, 2008).

Regular monitoring of frontal variations of the outlets of southeast Vatnajökull started in 1932 by Jón Eyþórsson and were later carried out by volunteers of the Icelandic Glaciological Society, providing annual records of the advance and retreat of the glaciers (Eyþórsson, 1963; Sigurðsson, 2013; http://spordakost.jorfi.is). The history of

Discussion Paper | Discussion Paper | Discussion Paper | Discussion Paper |
TCD
8, 4681–4735, 2014

retreat and volume changes of Hoffellsjökull since the end of the LIA has been derived from numerous archives (Aðalgeirsdóttir et al., 2011; Björnsson and Pálsson, 2004). Downwasting and volume loss of Kotárjökull (Fig. 1) in ~1890–2010 has been quantified by repeat photography and mapping of LIA glacial geomorphological features (Guðmundsson et al., 2012). The records of these two glaciers are integrated in our data base for comparison with the other outlets.

3 Data

3.1 Meteorological records

Long temperature and precipitation records are available from two lowland weather stations (Fig. 1) south of Vatnajökull; at Fagurhólsmýri (16 m a.s.l., 8 km south of Öræfajökull) and Hólar in Hornafjörður (16 m a.s.l., 15 km south of Hoffellsjökull). The temperature record at Hólar is available for the period 1884–1890 and since 1921, whereas, the precipitation measurements started in 1931 (Fig. 2). Temperature measurements started in 1898 at Fagurhólsmýri, and the precipitation record goes back to 1921 (Fig. 2). The temperature record has been extended back to the end of the 19th century by correlation with other temperature records from around the country, and the precipitation record by linear regression between temperature and precipitation of the local stations (see Aðalgeirsdóttir et al., 2011 for details). The mean summer temperature during the two warmest ten year periods of the measurement series at Hólar (1926–1936 and 2000–2010) was 10.3 °C and 10.5 °C respectively. For comparison the mean summer temperature for the time period 1884–1890 was 8.5 °C. Winter precipitation ranges between 800 and 1400 mm, and no long term trend is observed since start of measurements at the two stations. Precipitation has been measured at Kvísker (east of Öræfajökull) since 1963, and at Skaftafell (west of Öræfajökull) since 1964. The records from Kvísker show more than two times higher winter precipitation, and three times higher annual precipitation, than in Skaftafell (Fig. 2). This difference could

TCD
8, 4681–4735, 2014

be related to precipitation undercatch of the rain gauges especially during winter, but the underestimate is generally more pronounced for snow than rain (e.g., Sigurðsson, 1990).

3.2 Glacier geometry

The areal extent and the surface topography of the outlet glaciers at different times during the period ~ 1890–2010, has been derived from various data sets that are detailed in the following sub-chapters. The glacier margin has been digitized from maps and aerial images at various times for different glaciers.

3.2.1 LiDAR DEM

The most accurate DEMs of southeast Vatnajökull were produced with airborne LiDAR technology in late August–September 2010 and 2011 (Icelandic Meteorological Office and Institute of Earth Sciences, 2013). The high-resolution DEMs are 5 m × 5 m in pixel size with a < 0.5 m vertical and horizontal accuracy (Jóhannesson et al., 2013). The LiDAR DEMs provide a reference topography, used in constructing other glacier surface DEMs, for example in areas where corrections of contour lines from old paper maps have been necessary.

3.2.2 The LIA glacier surface topography

The surface topography at the LIA maximum ~ 1890 of the outlet glaciers of this study has previously been reconstructed from glacial geomorphological features (including lateral and terminal moraines, trimlines and erratics), historical photographs, and aerial images, using the LiDAR DEM as baseline topography (Hannesdóttir et al., 2014). The vertical accuracy of the ~ 1890 DEM is estimated to be around ±15–20 m.

3.2.3 Aerial images, maps and glacier surface data

The oldest reliable maps of the outlet glaciers are from the Danish General Staff (1 : 50 000), based on a trigonometrical geodetic surveys conducted in the summers of 1902–1904 (Danish General Staff, 1904). Considerable distortion was observed in the horizontal positioning, related to errors in the survey network established by the Danish Geodetic Institute (Böðvarsson, 1996; Pálsson et al., 2012). Less errors are found in the vertical component, revealed by comparison of the elevation of trigonometric points on mountain peaks and other definite landmarks between the LiDAR DEM and the 1904 maps (see also Guðmundsson et al., 2012). The maps do not cover all glaciers up to their ice divides. Lambatungnajökull was not surveyed in the early 20th century, but a manuscript map exists from 1938, based on a trigonometric geodetic survey and oblique photographs of the Danish General Staff (archives of the National Land Survey of Iceland). Only a small part of the terminus of Hoffellsjökull was surveyed in 1904, but a map from 1936 covers the whole glacier.

The AMS 1 : 50 000 maps with 20 m contour lines (Army Map Service, 1950–1951) cover all the outlet glaciers up to the ice divides, and are based on aerial photographs taken in August–September 1945 and 1946. The geometry in the upper parts of the glaciers, above ∼ 1100 m elevation, was based on the surveys of the Danish General Staff from the 1930s and 1940s, where contour lines are only estimates, indicating shape, not accurate elevation (see also Pálsson et al., 2012). The unpublished DMA maps from 1989 (Defense Mapping Agency, 1997) include only the eastern outlet glaciers. These maps were similarly derived by standard aerial photographic methods, based on images taken in August–September, with a scale of 1 : 50 000 and 20 m contour lines.

A Landsat satellite image of 2000 and aerial photographs from 1945, 1946, 1960, 1982 and 1989 (http://www.lmi.is/loftmyndasafn) and from 2002 (www.loftmyndir.is) were used to delineate the glacier margin and to estimate surface elevation changes in the accumulation area from the appearance of nunataks (isolated rock outcrops within the glaciers). A 20 m × 20 m DEM from Loftmyndir ehf., based on late summer aerial images from 2002, covers parts of Öræfajökull's outlet glaciers with vertical accuracy of < 5 m, excluding most of the accumulation areas. DGPS surface elevation measurements (with a vertical accuracy of 1–5 m) have been carried out during repeated mass balance surveys and radio echo sounding profiling in spring during the time period 2000–2003 on southeast Vatnajökull, and are used for DEM construction.

3.2.4 Bedrock topography

The bedrock topography has been derived from radio echo sounding measurements, carried out in the last two decades (Björnsson and Pálsson, 2004, 2008; Björnsson, 2009; Magnússon et al., 2007, 2012, and the data base of the Glaciological Group of the Institute of Earth Sciences, University of Iceland). We calculate the total ice volume from the bedrock DEMs and the relative ice volume changes as a fraction of the total volume. The accuracy of the bedrock measurements is ±5–20 m, depending on location.

4 Methods

4.1 Glacier surface DEMs

Glacier surface DEMs are used to determine changes in elevation and volume, and to infer mass changes (e.g., Reinhardt and Rentsch, 1986; Kääb and Funk, 1999). Comparison of DEMs retrieved from the aerial images of Loftmyndir ehf. 2002, SPOT5 HRS images in autumn from 2008 (Korona et al., 2009), and the 2010 LiDAR, reveals that the surface geometry in the upper accumulation area has undergone negligible changes during the first decade of the 21st century, at a time of rapid changes in the ablation area (see also Björnsson and Pálsson, 2008). Minor changes in the surface geometry in the upper accumulation area of a western outlet of Vatnajökull in 1998–2010 has similarly been observed (Auriac et al., 2014). When constructing the DEMs of

TCD
8, 4681–4735, 2014

1938, 1945, 1989 and 2002, it is therefore assumed that the glacier surface geometry in the upper reaches of the accumulation area does not change, but the estimated vertical displacement is superimposed on the LiDAR DEM.

The appearance of nunataks is used to determine ice surface elevation changes in the accumulation area of the southeast outlets, as has been used to estimate downwasting elsewhere (Paul et al., 2007; Rivera et al., 2007; Berthier et al., 2009; Pelto, 2010). The LiDAR DEMs are used as reference topography; the aerial images are laid on top of and georeferenced with a shaded relief LiDAR image. This provides new estimates on surface elevation changes in the upper reaches of the glaciers. Regular 50 m × 50 m DEMs were created by digitizing the contour lines of the paper maps (1904, 1938, 1945, 1989) and interpolated using kriging method (e.g., Wise, 2000). In upper parts of the glaciers, we extrapolated surface change data headward as a linear variation between available data points.

Due to lack of accurate contour lines in the highest part of the accumulation areas, we assume that ice divides are fixed in time, which may introduce an error in the areal extent. The ice divides are determined from the LiDAR DEM and the data base of the Glaciology Group of the Institute of Earth Sciences University of Iceland. The neighbouring surging outlets have affected the location of ice divides following surges (Björnsson et al., 2003). For example, the surges of Skeiðarárjökull 1991 and Dyngjujökull 1999 (Fig. 1), caused ice divides to shift on the order of a few hundred m; however the area affected is small compared to the total area of each outlet.

We consider the average vertical bias of each DEM to be smaller than the estimated point accuracy. Uncertainties related to the DEM reconstruction based on a few data points in the accumulation area, lead to minor errors in the estimated total volume change, since main volume loss occurs in the ablation areas. Uplift rates around Vatnajökull in the last 20 years have been on the order of 10–30 mm year^{-1}, highest around the edge of the ice cap (Árnadóttir et al., 2009; Auriac et al., 2013). We do not however, account for this change of the bedrock elevation in the most recent glacier surface DEMs, as it is smaller than the vertical error estimate.

4.1.1 DEMs of 1904 and 1938

The glacier margin delineated on the 1904 maps coincides with the LIA ∼ 1890 lateral moraines around an elevation of 400–500 m, thus surface lowering is assumed to only have taken place below that elevation during the cold time period ∼ 1890–1904 (see Hannesdóttir et al., 2014). A 1904 DEM of the terminus below 400–500 m was reconstructed and subtracted from the ∼ 1890 DEM (Hannesdóttir et al., 2014), to calculate volume changes for the time interval ∼ 1890–1904. Contour lines on the 1904 map indicate shape of the glacier surface geometry, not accurate elevation. The elevation of the trigonometric survey points on the glacier surface on the 1904 maps, serve as a base for generating the DEM, with an estimated vertical accuracy of 10–15 m. The contour lines of the manuscript map of 1938 of Lambatungnajökull were digitized, and their shape was adjusted according to the contours of the AMS 1945 map.

4.1.2 DEMs of 1945

Due to the errors in the old trigonometric network for Iceland, parts of the 1945 maps are somewhat distorted horizontally. Sections of the scanned maps were thus georeferenced individually, by fitting each map segment to the surrounding valley walls, using the LiDAR as reference topography. To estimate glacier surface elevation changes in the accumulation area between 1945 and 2010, we compared the size of nunataks on the original aerial images and the LiDAR shaded relief images (an example shown in Fig. 3). No difference in surface elevation was observed above 1300–1400 m, wherefrom the LiDAR DEM was added to create a continuous 1945 DEM. The glacier margin was revised by analysing the original aerial images, for example in areas where shadows had incorrectly been interpreted as bedrock or snow-covered gullies and valley walls as glacial ice. A conservative vertical error estimate of 5–10 m is estimated for the 1945 DEM.

4.1.3 DEMs of 1989

DEMs from the contour lines of the DMA unpublished maps of the eastern outlets have previously been created at the Institute of Earth Sciences, University of Iceland. But here some adjustments were made to the glacier surface geometry in the upper accumulation area, by comparing the size of the nunataks on the original aerial images with the shaded relief image of the LiDAR DEM. The glacier outline was also reassessed from the original aerial images. A conservative vertical error of 5 m for the 1989 DEM is estimated, based on experience of interpreting the DMA maps of Icelandic glaciers (Guðmundsson et al., 2011; Pálsson et al., 2012).

4.1.4 DEMs of 2002

Negligible surface elevation changes above 1300–1400 m are observed between the aerial images of Loftmyndir ehf. from 2002 and the shaded relief of the 2010 LiDAR DEM; thus the high-resolution DEM was mosaiced (above that elevation) to create a complete 2002 DEM. Comparison of altitude in ice free areas bordering the glaciers, from the LiDAR and the Loftmyndir ehf. DEMs, reveals a vertical bias of 2–5 m. The glacier surface elevation in the accumulation area was verified by spring DGPS measurements from radio echo sounding survey transects from the same year. The glacier margins of the Öræfajökull outlet glaciers were digitized from the high-resolution aerial images of Loftmyndir ehf, whereas the glacier margin of the eastern outlets were digitized from Landsat satellite images from 2000 (http://landsat.usgs.gov).

A 2002 DEM of the eastern outlet glaciers was constructed from a series of DGPS measurements from survey transects of radio echo sounding measurements in the time period 2000–2003. The LiDAR DEM was used as topographical reference. The spring DGPS elevation measurements in the accumulation area were corrected by subtracting the difference between spring and autumn elevation from the measured surface, to retrieve an autumn DEM. Seasonal changes in glacier surface elevation amount to 5 m on average in the accumulation area, observed at mass balance stakes on southeast Vatnajökull every autumn and spring during the period 1996–2010. The vertical error estimate for the 2002 DEM is approximately 1–2 m.

4.2 Glacier hypsometry

The hypsometry (area distribution with altitude) of individual glaciers plays an important role in their response to climate change through its link with mass-balance elevation distribution (e.g., Furbish and Andrews, 1984; Oerlemans et al., 1998). The hypsometry is determined by bedrock topography, ice thickness, and ice volume distribution (e.g., Marshall, 2008; Jiskoot et al., 2009). One of the first people to descibe the hypsometry of glaciers and classify the hypsometric curves was Ahlmann (in Lliboutry, 1956). The hypsometric curves of the outlets of southeast Vatnajökull were generated from the LiDAR DEM and ~ 1890 DEM by creating histograms of the elevation data with 50 m elevation intervals.

4.3 ELA derived from MODIS imagery and the LiDAR DEMs

The elevation of the snowline at the end of summer provides an estimate for the ELA on temperate glaciers (e.g., Östrem, 1975; Cuffey and Paterson, 2010). In recent years satellite data have been used to estimate the ELA by this approximation in remote regions and where mass balance is not measured (e.g., Barcaza et al., 2009; Mathieu et al., 2009; Mernild et al., 2013; Rabatel et al., 2013; Shea et al., 2013). Since limited mass balance measurements exist for the outlet glaciers of this study (Fig. 1), the snowline retrieved from the MODIS images is a useful proxy for the present day ELA. The snowline was digitized and projected over the LiDAR DEMs to obtain the elevation. The average snowline elevation and standard deviation was calculated for the glaciers from each image. The accumulation area ratio (AAR) of the outlet glaciers was estimated from the average snowline elevation from all years and the glacier margin in 2010.

4.4 Volume calculations and average geodetic mass balance

Ice volume changes for the different time periods since the end of the LIA until 2010 were obtained by subtracting the DEMs from each other. Given the bedrock DEMs, the fraction of the volume loss (of the total volume) is calculated. The ice volume change is converted to average annual mass balance, bn, expressed in m of water equivalent per year (m w.e. a^{-1}) averaged over the mean glacier area

$$\text{bn} = \frac{\rho \times \Delta V}{A \times \Delta t} \tag{1}$$

where ρ is the average specific density of ice, 900 kg m^3 (Sorge's law), ΔV the volume change, A the average of the initial and final glacier area and Δt the time difference in years between the two DEMs. The volume change is the average elevation change (Δh) between two years, multiplied by the area of the glacier,

$$\Delta V = \Delta h \times A \tag{2}$$

The uncertainty related to the conversion of ice volume to mass change to obtain geodetic mass balances, is small for long periods (decades) of glacier retreat, and when volume loss is mainly confined to the ablation area, mostly ice is lost (e.g., Bader, 1954; Huss, 2013). We base our estimates of the error for the geodetic mass balance on previous assessments of errors in DEM reconstruction and geodetic mass balance calculations for ice caps in Iceland (Guðmundsson et al., 2011; Pálsson et al., 2012).

5 Results

5.1 Spatial and temporal variability of the ELA

Spatial variability is observed in the ELA deduced from the 2007–2011 MODIS images. The average ELA and the standard deviation for each year is displayed in Fig. 4.

TCD
8, 4681–4735, 2014

The ELA of the western outlet glaciers of Öræfajökull is approximately 170 m higher than on the eastern outlet glaciers, and the ELA rises eastward from Skálafellsjökull to Lambatungnajökull by ~ 200 m. Due to the low resolution of the MODIS images, the snowline on the narrow outlet glaciers of Öræfajökull (Morsárjökull, Svínafellsjökull, Kotárjökull, Kvíárjökull, and Hrútárjökull) is only discernible on a limited number of images. The snowline on the ~ 2 km wide Skaftafellsjökull and ~ 3.5 km wide Fjallsjökull is detectable on several images, allowing determination of the ELA in all years. The ELA range and AAR of the narrow outlet glaciers of Öræfajökull, is thus inferred by comparison with the neighbouring glaciers during overlapping years (Table 1). The ELA fluctuated by 100–150 m during this 5 years period. A similar interannual trend of the ELA is observed; the ELA in 2009 is the lowest for most of the glaciers, whereas the ELA in 2010 is usually the highest (Fig. 4). The AAR of the outlet glaciers ranges between 0.43 and 0.71, but the majority have an AAR of 0.6–0.65 (Table 1).

5.2 Frontal variations and areal change

The areal extent of the outlet glaciers at different times is shown in Figs. 5 and 6, and in Table 2. The outlets started retreating from their terminal LIA moraines ~ 1890, (Hannesdóttir et al., 2014), and had retreated 1–4 km by 2010 (Figs. 7 and 8), corresponding to an areal decrease of 164 km^2, equal to 16 % of the ~ 1890 areal extent, and in the range of 15–30 % for individual glaciers (Table 2 and Fig. 9). Main area decrease occurred in the ablation area, although small glacier tongues at higher elevation did also retreat in the 20th century (Figs. 5 and 6). Most glaciers had by 1945 lost 10 % of their ~ 1890 area (Table 2), and the rate of area loss was the highest during the time period 1904–1945 for majority of the glaciers (Fig. 10a). Hrútárjökull had by that time lost 17%, however its debris covered terminus on the 1945 aerial image prevents accurate interpretation of the glacier margin. In the following few decades glacial retreat slowed down or halted (Fig. 7). During the time period 1982/1989–2002 the areal extent of the glaciers changed little (Figs. 5, 6 and 7 and Table 2). Morsárjökull, Skaftafellsjökull, Hrútárjökull, Skálafellsjökull and Fláajökull advanced in 1970–1990, others remained stagnant (Fig. 7). The terminus position of Skálafellsjökull, Heinabergsjökull and Fláajökull was not measured during this time period, but from aerial images of 1979, it was possible to delineate the location of the termini, and infer about their slight advances based on the single year data point (Fig. 7). The majority of the glaciers started retreating just prior to the turn of the 21st century; between 2002 and 2010 the glaciers experienced high rates of area loss, the highest for Heinabergsjökull and Hoffellsjökull during the last 120 years (Fig. 10a and Table 2).

5.3 Thinning and volume changes

Between ~ 1890 and 2010 the outlet glaciers lowered by 150–270 m near the terminus, but negligible downwasting was observed above ~1500–1700 m elevation (Fig. 11a). Svínafellsjökull and Kvíárjökull underwent the smallest surface lowering during this period, whereas Heinabergsjökull, Hoffellsjökull and Lambatungnajökull experienced the greatest downwasting (Fig. 11a). Surface lowering between 1945 and 2010 is shown in Fig. 11b. The comparison of the size of nunataks in the upper reaches of the outlet glaciers, reveals negligible surface elevation change above 1300 m a.s.l. An example of the different appearance of nunataks in the 20th century is shown in Fig. 3 of the outcrops of Skaftafellsjökull called "Skerið milli skarða". Across the whole southeast part of Vatnajökull, the nunataks are smaller in area in 1989 and 1982 than in 1945 or 2002, meaning that the glacier was thicker at that time. A slight thickening in the accumulation area between 1945 and 1982/1989 is thus inferred. The similar size of the nunataks in 1945 and 2002 is evident.

In the time period ~ 1890–2010 the outlets collectively lost 60 ± 8 km^3 (around 22 % of their LIA volume) and the relative volume loss of individual outlets was in the range of 15–50 % (Table 3 and Fig. 9). The rate of volume loss was highest between 2002 and 2010 and second highest in the time period 1904–1945 (Fig. 10b). All glaciers had lost at least half of their post-LIA volume loss by 1945 (Table 3). The eastern outlet glaciers (except Lambatungnajökull), experienced higher rates of volume loss than majority of the smaller and steeper outlets of Öræfajökull ice cap during every

TCD
8, 4681–4735, 2014

period of the last 120 years (Fig. 10b). For example between 2002 and 2010 the volume loss of the Öræfajökull outlets was in the range of −0.34 to −0.13 $km^3\,a^{-1}$ vs. −0.95 to −0.28 $km^3\,a^{-1}$ of the eastern outlets (Fig. 10b). The lack of 1980s DEMs of the Öræfajökull outlets, restricts the comparison with the eastern outlet glaciers to the time period 1945–2002.

5.4 Geodetic mass balance

The geodetic mass balance of all glaciers was negative during every time interval of the study period (Fig. 12 and Table 4). The average mass balance of the outlets ∼ 1890–2010 was −0.38 m w.e. a^{-1}, and in the range of −0.70 to −0.32 m w.e. a^{-1} for individual outlets. The mass loss in ∼ 1890–1904 was between −0.5 and −0.15 m w.e. a^{-1}. In the first half of the 20th century (1904–1945), the average mass balance was in the range of −1.00 to −0.50 m w.e. a^{-1}. The geodetic mass balance during the warmest decade of the 20th century (1936–1945), is only available for Hoffellsjökull and Lambatungnajökull, when they lost 1.00 and 0.75 m w.e. a^{-1}, respectively. In 1945–2002 the mass balance returned to similar values as at the turn of the 19th century. The geodetic mass balance of the eastern outlets was similar during the periods 1945–1989 and 1989–2002. The most negative balance is estimated in 2002–2010, ranging between −1.50 and −0.80 m w.e. a^{-1}, except Heinabergsjökull which lost on average −2.70 m w.e. a^{-1}.

Fjallsjökull and Hrútárjökull experienced the most negative average mass balance during the majority of the time periods of the Öræfajökull outlets (Fig. 12). Heinabergsjökull and Hoffellsjökull sustained the highest rate of mass loss of the eastern outlets during most intervals. Skálafellsjökull and Fláajökull generally had the least negative mass balance during every time period of the post-LIA interval of the eastern outlet glaciers, and Kvíárjökull and Svínafellsjökull of the Öræfajökull outlets.

5.5 Glacier hypsometry

The outlet glaciers of southeast Vatnajökull are divided into 5 hypsometric classes adopted from the categorization of De Angelis (2014), first proposed by Osmaston (1975) and also presented in Furbish and Andrews (1984):

- (A) Glaciers with a uniform hypsometry, i.e. area is constant with elevation
- (B) Glaciers where the bulk of the area lies above the ELA
- (C) Glaciers where the bulk of the area lies below the ELA
- (D) Glaciers where the bulk of the area lies at the ELA
- (E) Glaciers with bimodal hypsometric curves, where the ELA lies approximately between two peaks

The majority of the studied glaciers belong to shape class B (Table 1 and Fig. 13). Lambatungnajökull and Hrútárjökull belong to shape class D. Two glaciers have bimodal hypsometric curves (class E), Svínafellsjökull and Fjallsjökull, the latter could be classified as a piedmont glacier (class C) in its greatest extent.

6 Discussion

6.1 Glacier changes since the end of the LIA

Retreat of the outlet glaciers of southeast Vatnajökull from the LIA terminal moraines, that started in the last decade of the 19th century, was not continuous. The recession accelerated in the 1930s, as a result of the rapid warming beginning in the 1920s (Figs. 2b and 7). Glacier recession slowed down following cooler summers after 1940s, and from the 1960s to late 1980s the glaciers remained stagnant or advanced slightly (Fig. 7). A mass gain in the accumulation area during this cooler period was recognized on the aerial images of the 1980s, by smaller nunataks than on the 1945 aerial images (Fig. 3). The mass balance of the outlets in some years of the 1970s and 1980s may have been positive, although the geodetic mass balance of 1945–1989 (of the eastern outlets) and 1945–2002 (Öræfajökull outlets) was negative. The mass balance of the larger ice caps in Iceland was generally close to zero in 1980–2000 (e.g., Guðmundsson et al., 2009, 2011; Aðalgeirsdóttir et al., 2006, 2011). According to in situ measurements, mass balance was positive on Vatnajökull 1991–1994, but negative since then (Björnsson and Pálsson, 2008; Björnsson et al., 2013). Warmer temperatures after the mid-1990s (Fig. 2b) caused retreat of the southeast outlets, that increased after year 2000 (Björnsson and Pálsson, 2008; Björnsson et al., 2013). The rate of volume and mass loss was highest during the period 2002–2010 for almost all the southeast outlet glaciers (Figs. 10b and 12, Table 4). The geodetic mass balance is in line with the measured specific mass balance of Breiðamerkurjökull and Hoffellsjökull, which was on average $-1.4\,\mathrm{m\,w.e.\,a^{-1}}$ (Björnsson et al., 2013). Langjökull ice cap, similarly experienced high rates of mass loss in the period 1997–2009 ($-1.26\,\mathrm{m\,w.e.\,a^{-1}}$), which was however, even more negative in the warm decade of 1936–1945 (Pálsson et al., 2012).

Increasing negative mass balance in recent years from majority of ice sheets, ice caps and glaciers worldwide is reported in the latest IPCC report (Vaughan et al., 2013, and references therein). Glaciers in the Alps (Huss, 2012) and in Alaska (Luthcke et al., 2008) lost on average $1.0\,\mathrm{m\,w.e.\,a^{-1}}$ during the first decade of the 21st century, considerably smaller than the mass loss of glaciers in Iceland (Fig. 12b), which experienced among the most negative mass balance worldwide in the early 21st century (Vaughan et al., 2013). In this time period increased surface lowering on the southeast outlets of Vatnajökull is evidenced in emerging rock outcrops and expansion of nunataks up to an elevation of approximately 1200 m. The pattern of increased downwasting in accumulation areas in recent years has been observed in Alaska (Cox and March, 2004), the Alps (Paul et al., 2004), North Cascade glaciers (Pelto, 2010), and Svalbard (James et al., 2012).

The amount of ice (in km^3) lost from the outlets of southeast Vatnajökull ∼ 1890–2010 equals the estimated ice loss of Langjökull and Breiðamerkurjökull during the same time interval (Pálsson et al., 2012; Guðmundsson, 2014). The average mass balance of the outlets in this time period was $-0.38\,\text{m w.e. a}^{-1}$, compared to $-0.45\,\text{m w.e. a}^{-1}$ of Langjökull (Pálsson et al., 2012) and $-0.64\,\text{m w.e. a}^{-1}$ of Breiðamerkurjökull (Guðmundsson, 2014). For comparison glaciers in the Alps have lost on average $-0.31\,\text{m w.e. a}^{-1}$ since the end of the LIA (Huss, 2012), which is 25 % less than the mass loss of the southeast outlets of Vatnajökull.

In situ mass balance measurements of glaciers in Iceland and degree-day mass balance models of selected glaciers indicate that the mass balance is governed by variation in summer ablation (which is strongly correlated with temperature), rather than winter accumulation (Björnsson and Pálsson, 2008; Guðmundsson et al., 2009, 2011; Pálsson et al., 2012; Björnsson et al., 2013). Higher than average winter precipitation at the meteorological stations south of Vatnajökull, is not correlated with more positive geodetic mass balances of the southeast outlets. However, a strong correlation ($r = 0.94$–0.98) is found between the geodetic mass balance and the average summer temperature (Table 4). Temperature records in Iceland indicate a warming of approximately 1.5 °C since the latter part of the 19th century until 2002 (Hanna et al., 2004; Jóhannesson et al., 2007). The mean annual temperature has been ∼ 1 °C higher after 2000 than in the mid-1990s, which is 3–4 times higher than the average warming of the Northern Hemisphere during the same time interval (Jones et al., 2012).

The ELA of the outlets of southeast Vatnajökull has since the end of the LIA, risen by > 300 m; the ELA during the LIA maximum has been inferred from the elevation of the highest up-valley lateral LIA moraines of the studied glaciers (Hannesdóttir et al., 2014). Similar spatial differences in the ELA at both time periods have been observed, a 150–200 m difference between the western and eastern outlets of Öræfajökull, and increasing ELA from Skálafellsjökull to Lambatungnajökull. The geographical variability of the ELA is likely related to orographically enhanced precipitation on the SE coast (e.g., Crochet et al., 2007; Rögnvaldsson et al., 2007).

6.2 Different response to similar climate forcing

The meteorological records from Hólar in Hornafjörður and Fagurhólsmýri indicate similar temperature and precipitation fluctuations during the 20th and early 21st century at both stations since start of measurements (Fig. 2). We thus infer that the studied outlets have experienced similar climate forcing since the end of the LIA. The precipitation records from the lowland stations indicate little variation during this time period. Glaciers respond to mass balance changes by adjusting their surface elevation and area. Our results show that glaciers with different hypsometry respond dynamically differently to the same climate forcing as has been reported from several studies (e.g., Kuhn et al., 1985; Oerlemans et al., 1998; Oerlemans, 2007; Jiskoot et al., 2009; Davies et al., 2012; De Angelis, 2014). Glaciers of shape class B lost the smallest percentage of their ~ 1890 volume (15–20%); except Heinabergsjökull (30%) and Hoffellsjökull (25%). Heinabergsjökull has a small peak in the area distribution in the ablation area (Fig. 13), and the peak in the area distribution of Hoffellsjökull is close to the modern average ELA. Lambatungnajökull and Hrútárjökull that are of shape class D, have lost 40 % and 50 % of their ~ 1890 volume, respectively. The two glaciers with bimodal hypsometric curves (class E), Svínafellsjökull and Fjallsjökull, have lost 30 % and 35 % of their ~ 1890 volume, respectively.

There is a noticeable difference in the response of the neighbouring outlet glaciers, Skaftafellsjökull and Svínafellsjökull. The former has retreated 2.7 km and lost 20 % of its ~ 1890 volume, whereas the latter has only retreated 0.8 km and lost 30 % of its ~ 1890 volume although part of the surface lowering may be due to excavation of the bed, creating an overdeepening in the terminus area of the glacier, as is well known for Breiðamerkurjökull (Björnsson, 1996). Similar difference is observed between Skálafellsjökull and Heinabergsjökull, where the former glacier lost 15 % of its ~ 1890 volume and retreated 2 km, and the latter lost 30 % of its ~ 1890 volume and retreated 3 km. Their bedrock topography is different (Fig. 8), and part of the surface

TCD
8, 4681–4735, 2014

lowering in the ablation area of Heinabergsjökull may likewise be attributed to excavation of the bed.

The area-altitude distribution of a glacier controls its sensitivity to a rise in the ELA. For example, a temperature rise of 0.5–1.0 °C would raise the ELA by approximately 100 m. The ablation area of the gently sloping eastern outlet glaciers will expand more than for the majority of the steeper Öræfajökull outlets following a rise in the ELA. Lambatungnajökull would almost loose its accumulation area, Hoffellsjökull and Morsárjökull would loose approximately 30 and 45 %, respectively, whereas the accumulation area of Fjallsjökull would only decrease by 7%.

A clearer distinction between the response of the Öræfajökull outlets and the eastern outlets to the post-LIA climate perturbations would perhaps be expected, as steeper glaciers generally respond faster to changes in climate (e.g., Cuffey and Paterson, 2010). The thinner Öræfajökull glaciers, with ice divides lying 400–500 m higher than on the eastern outlet glaciers and steep mass balance gradient, are suspected to have a shorter response time. The response time of a glacier, the time it takes for a glacier to adjust its geometry to a new steady state after a change in mass balance, is a function of its mean thickness and terminus ablation (Jóhannesson et al., 1989), and of its hypsometry and mass balance gradient (Cuffey and Paterson, 2010). However, the geodetic mass balance records and terminus fluctuations of the outlets of southeast Vatnajökull do not indicate a distinct difference in the response of the outlets of the two glaciated regions. But the temporal resolution of the geodetic mass balance records is lower than the supposed response time of 15–30 years, given terminus ablation of $-10\,\mathrm{m\,w.e.\,a^{-1}}$ and average ice thicknesses of 150–300 m. In order to detect mass balance changes during the colder period following the 1960s, aerial images could be used to construct surface DEMs, and thereby increase the temporal resolution of the mass balance record for the period 1945–1989/2002.

Glacier surface lowering is influenced by the geometry and hypsometry of the outlet glaciers, and the proglacial lakes. Surface lowering is generally a function of elevation (Fig. 11), but the downwasting near the terminus is highly variable. Two of the glaciers experiencing the greatest surface lowering near the termini (Heinabergsjökull and Lambatungnajökull), are constrained by valley walls on both sides, and have retreated close to 3 km in the post-LIA period (Table 1). The surface elevation changes near the terminus of Svínafellsjökull and Kvíárjökull are in the lower range (Fig. 11). The glaciers only retreated about 1 km in ~ 1890–2010 (Fig. 7), and they are both confined by steep valley walls and terminate in overdeepened basins. Their mass loss has been governed by thinning rather than retreat, which may be related to their bedrock topography. Using simplified dynamical models, Adhikari and Marshall (2013) found that valley glaciers with overdeepened beds were likely to withdraw through deflation more than marginal retreat.

6.3 Volume-area scaling

Less than 0.1 % of the world's glacier volume is known (Bahr, 1997) and observations of volume evolution are rare (e.g., Flowers and Clarke, 1999; Radic et al., 2007; Möller and Schneider, 2010). Glacier volume change estimates of the whole post-LIA time period are limited (Vaughan et al., 2013, and references therein), and results of model studies are often compared with calculations from other models, not with observations (e.g., Oerlemans, 2007). Our volume-area time series of the 12 outlets of southeast Vatnajökull starts at the end of the LIA, when most of the glaciers had reached their maximum size in historical times, some even since the end of the early Holocene deglaciation (Thórarinsson, 1943). From glacier area inventories, glacier volume has been estimated by applying scaling relations (e.g., Chen and Ohmura, 1990; Bahr, 1997) and ice-dynamical considerations (e.g., Adhikari and Marshall, 2013). Our data set provides an opportunity to evaluate the empirical and modelled volume-area scaling relation. The volume-area scaling method assumes that the volume of a glacier is proportional to its area in a power γ

$$V = c \times A^{\gamma} \quad (3)$$

TCD
8, 4681–4735, 2014

where V and A are the volume and surface area of a single glacier, and c and γ are constants. Based on statistical regression of data from 63 mountain glaciers, Chen and Ohmura (1990) found γ to be close to 1.36, whereas theoretical considerations predict a value of 1.375 for valley glaciers, supported with data from 144 glaciers (Bahr et al., 1997). The volume-area evolution of the last 120 years of each studied glacier of southeast Vatnajökull is plotted in Fig. 14. The scaling constants are estimated for the years ~1890, 1904, 1945, 2002, 2010; γ ranging from 1.357 to 1.457, and c between 0.030 and 0.048 (Table 5).

The scaling parameters are expected to evolve over time; as the glaciers retreat, γ decreases due to the fact that glaciers thin before they undergo notable area decrease (e.g., Radic et al., 2007; Adhikari and Marshall, 2012). Adhikari and Marshall (2012) show how different topographic and climatic settings, glacier flow dynamics, and the degree of dis-equilibrium with climate systematically affect the volume-area relation. The magnitude of γ after 100 years of glacier retreat was found to be 1.377 ± 0.063, comparable with $\gamma = 1.357$ calculated for a sample of real alpine glaciers (Chen and Ohmura, 1990). The steady state exponent was however 1.46 (Adhikari and Marshall, 2012). From our data set this trend is not evident, as the volume-area data set of ~1890 gives $\gamma = 1.357$, compared to 1.457 in 2002 (Table 5). As seen in Fig. 14, the volume-area relation of the individual outlets varies. Glaciers with bulk of their area distribution above the ELA (shape class B) are in line with the slope of the classical volume-area relation of Bahr et al. (1997) and Adhikari and Marshall (2012) as well, with a slightly higher value for the coefficient c. The majority of the outlets belonging to other hypsometric classes (Hrútárjökull, Svínafellsjökull, Lambatungnajökull, Fjallsjökull, Hoffellsjökull and Heinabergsjökull) experienced larger relative volume loss, have a larger exponent γ (Fig. 14), and lost volume at a faster rate than the shape class B glaciers. The increase in γ from our data set can probably be explained by the variable response of individual outlet glaciers and the glaciers not being in the same transient states at each point in time. Furthermore our data set may not be not large enough to make estimates on the change of γ. Comparison of the ice volume calcu-

TCD
8, 4681–4735, 2014

lated according to the exponents of Bahr et al. (1997) and Adhikari and Marshall (2012) with our volume estimates, reveals an underestimate in ice volume of up to 50 %. The variable hypsometry, shape, size, and thickness of the outlets of southeast Vatnajökull, indicate that the coefficients of the power law relating glacier volume and area need to be adjusted to variable glaciological parameters and can only be used in a statistical way on a large number of glaciers when inferring the volume from measured area.

7 Conclusions

We have compiled a series of glacier outlines and glacier surface DEMs of the outlets of southeast Vatnajökull from various sources. The multi-temporal glacier inventory of volume and area changes for the period ∼ 1890–2010 is unique. We derive the mass balance history of one of the most sensitive glaciated areas in the world for the post-LIA period by geodetic methods. The average mass balance during the period 1890–2010 was −0.38 m w.e. a^{-1}. The glaciers are sensitive to climate change, with high mass turnover rates, and experienced among the highest rates of mass loss (on average 1.34 m w.e. a^{-1}) worldwide in the early 21st century (Vaughan et al., 2013). The glaciated area decreased by 162 km^2 in ∼ 1890–2010, and the outlets collectively lost 60 ± 8 km^3 of ice, contributing 0.154 ± 0.02 mm to sea level rise in the post-LIA period.

Each glacier lost between 15 and 50 % of their ∼ 1890 volume, the difference attributed to their variable hypsometry and bedrock topography, and the presence of proglacial lakes, that enhance melting at the terminus. The different response of glaciers experiencing similar climatic forcing, underlines the importance of a large sample of glaciers when interpreting the climate signal, and highlights once more the effect of glacier hypsometry and geometry on the dynamic response of glaciers to changes in mass balance. The dynamically different response of the glaciers show, that frontal variations and aera changes only provide limited information on the glacier response to climate perturbations, as some experience rapid downwasting but little retreat.

TCD
8, 4681–4735, 2014

A ~ 200 m difference of the ELA of the outlets glaciers was observed during the time period 2007–2011, presumably due to spatial differences in orographically enhanced precipitation, associated with atmospheric fronts and cyclones. The ELA has risen > 300 m since the end of the 19th century. The steep Öræfajökull outlet glaciers are more likely to survive future warming, since their ice divides are 400–500 m higher than the eastern outlets. Furthermore, proglacial lakes will increase in size and new will form as the glaciers retreat, and enhance melting.

From the data set of the variations of the outlets of southeast Vatnajökull we have assessed the power-law relation between glacier area and volume. A comparison of the ice volume between our measurements and the estimates based on the constants used by Bahr et al. (1997) and Adhikari and Marshall (2012), shows that the relation could underestimate the ice volume up to 50%. This needs to be taken into account, since glaciers outside the polar areas are contributing to sea level rise at an accelerated rate. Furthermore, the glacier inventory provides information that can be used to calibrate mass balance-ice flow models that simulate future glacier response to climate scenarios. Work is already underway to simulate the 20th century evolution of three of the eastern outlets.

Acknowledgements. This work was funded by a doctoral grant of the Research Fund of the University of Iceland to Hrafnhildur Hannesdóttir, two additional grants from the Research Fund to Guðfinna Aðalgeirsdóttir, the Icelandic Road Administration, The Nordic Centre of Excellence SVALI, the Kvísker Fund, the University of Iceland's Research Centre in Hornafjörður, and the Directorate of Labour. We thank Trausti Jónsson at the Icelandic Meteorological Office for access to the temperature and precipitation records. The 2010 LiDAR DEM was acquired as a part of an ongoing collective effort between the Icelandic Meteorological Office and the Institute of Earth Sciences of the University of Iceland, to map the surface topography of Icelandic ice caps, initiated in the International Polar Year 2007–2009. We thank Tómas Jóhannesson for very helpful comments on an early draft of the manuscript. This publication is contribution No. 42 of the Nordic Centre of Excellence SVALI, "Stability and Variations of Arctic Land Ice", funded by the Nordic Top-level Research Initiative (TRI).

References

Aðalgeirsdóttir, G., Guðmundsson, G. H., and Björnsson, H.: Volume sensitivity of Vatnajökull Ice Cap, Iceland, to perturbations in equilibrium line altitude, J. Geophys. Res.-Earth, 110, F04001, doi:10.1029/2005jf000289, 2005. 4685

Aðalgeirsdóttir, G., Jóhannesson, T., Björnsson, H., Pálsson, F., and Sigurðsson, O.: Response of Hofsjökull and southern Vatnajökull, Iceland, to climate change, J. Geophys. Res.-Earth, 111, F03001, doi:10.1029/2005JF000388, 2006. 4683, 4685, 4699

Aðalgeirsdóttir, G., Guðmundsson, S., Björnsson, H., Pálsson, F., Jóhannesson, T., Hannesdóttir, H., Sigurðsson, S. Þ., and Berthier, E.: Modelling the 20th and 21st century evolution of Hoffellsjökull glacier, SE-Vatnajökull, Iceland, The Cryosphere, 5, 961–975, doi:10.5194/tc-5-961-2011, 2011. 4683, 4685, 4686, 4699, 4717, 4722

Adhikari, S. and Marshall, S. J.: Glacier volume-area relation for high-order mechanics and transient glacier states, Geophys. Res. Lett., 39, doi:10.1029/2012gl052712, 2012. 4704, 4705, 4706, 4735

Adhikari, S. and Marshall, S. J.: Influence of high-order mechanics on simulation of glacier response to climate change: insights from Haig Glacier, Canadian Rocky Mountains, The Cryosphere, 7, 1527–1541, doi:10.5194/tc-7-1527-2013, 2013. 4703

Army Map Service, C. o. E.: Series C762, sheets: 6018-I,IV, 6019-I,II,III,IV, 6020-I,II,III, 611IV, 6120-I,II,III, US Army, Washington D.C., 1950–1951. 4688

Árnadóttir, T., Lund, B., Jiang, W., Geirsson, H., Björnsson, H., Einarsson, P., and Sigurðsson, T.: Glacial rebound and plate spreading: results from the first countrywide GPS observations in Iceland, Geophys. J. Int., 177, 691–716, doi:10.1111/j.1365-246X.2008.04059.x, 2009. 4690

Auriac, A., Spaans, K. H., Sigmundsson, F., Hooper, A., Schmidt, P., and Lund, B.: Iceland rising: Solid Earth response to ice retreat inferred from satellite radar interferometry and visocelastic modeling, J. Geophys. Res.-Sol. Ea., 118, 1331–1344, doi:10.1002/Jgrb.50082, 2013. 4690

Auriac, A., Sigmundsson, F., Hooper, A., Spaans, K. H., Björnsson, H., Pálsson, F., Pinel, V., and Feigl, K. L.: InSAR observations and models of crustal deformation due to glacial surge in Iceland, Geophys. J. Int., 198, 1329–1341, 2014. 4689

Bader, H.: Sorge's Law of densification of snow on high polar glaciers, J. Glaciol., 2, 319–323, 1954. 4694

TCD
8, 4681–4735, 2014

Area, volume and mass changes of southeast Vatnajökull ice cap

Hannesdóttir et al.

Bahr, D. B.: Global distributions of glacier properties: A stochastic scaling paradigm, Water Resour. Res., 3, 1669–1679, doi:10.1029/97WR00824, 1997. 4703, 4735
Bahr, D. B., Meier, M. F., and Peckham, S. D.: The physical basis of glacier volume-area scaling, J. Geophys. Res.-Sol. Ea., 102, 20355–20362, doi:10.1029/97jb01696, 1997. 4704, 4705, 4706
Barcaza, G., Aniya, M., Matsumoto, T., and Aoki, T.: Satellite-Derived Equilibrium Lines in Northern Patagonia Icefield, Chile, and Their Implications to Glacier Variations, Arct. Antarct. Alp. Res., 41, 174–182, doi:10.1657/1938-4246-41.2.174, 2009. 4693
Bauder, A., Funk, M., and Huss, M.: Ice-volume changes of selected glaciers in the Swiss Alps since the end of the 19th century, Ann. Glaciol., 46, 145–149, 2007. 4683
Berthier, E., Le Bris, R., Mabileau, L., Testut, L., and Remy, F.: Ice wastage on the Kerguelen Islands (49 degrees S, 69 degrees E) between 1963 and 2006, J. Geophys. Res.-Earth, 114, doi:10.1029/2008JF001192, 2009. 4690
Björnsson, H.: Glaciers in Iceland, Jökull, 29, 74–80, 1979. 4685
Björnsson, H.: Scales and rates of glacial sediment removal: a 20 km long and 300 m deep trench created beneath Breiðamerkurjökull during the Little Ice Age, Ann. Glaciol., 22, 141–146, 1996. 4701
Björnsson, H.: Jöklar á Íslandi, Opna, Reykjavík, 2009. 4685, 4689
Björnsson, H., and Pálsson, F.: Jöklar í Hornafirði, rannsóknir og saga, in: Jöklaveröld, Náttúra og Mannlíf, edited by: Björnsson, H., 125–164, Skrudda, Reykjavík, 2004. 4686, 4689
Björnsson, H., and Pálsson, F.: Icelandic glaciers, Jökull, 58, 365–386, 2008. 4684, 4685, 4689, 4699, 4700
Björnsson, H., Pálsson, F., Sigurðsson, O., and Flowers, G. E.: Surges of glaciers in Iceland, Ann. Glaciol., 36, 82–90, 2003. 4690
Björnsson, H., Pálsson, F., Guðmundsson, S., Magnússon, E., Aðalgeirsdóttir, G., Jóhannesson, T., Berthier, E., Sigurðsson, O., and Thorsteinsson, T.: Contribution of Icelandic ice caps to sea level rise: Trends and variability since the Little Ice Age, Geophys. Res. Lett., 40, 1546–1550, doi:10.1002/Grl.50278, 2013. 4683, 4685, 4699, 4700
Böðvarsson, A.: Landmælingar og kortagerð Dana á Íslandi: Upphaf landmælinga á Íslandi, Landmælingar Íslands, Reykjavík, 1996. 4688
Chen, J. and Ohmura, A.: Estimation of Alpine glacier water resources and their change since the 1870s, IAHS (International Association of Hydrological Sciences), 193, 127–135, 1990. 4703, 4704

Church, J. A., Clark, P. U., Cazenave, A., Gregory, J. M., Jevrejeva, S., Levermann, A., Merrifield, M. A., Milne, G. A., Nerem, R. S., Nunn, P. D., Payne, A. J., Pfeffer, W. T., Stammer, D., and Unnikrishnan, A. S.: Sea level change, in: Climate Change 2013: The Physical Science Basis. Contribution of Working Group I to the Fifth Assessment Report of the Intergovernmental Panel on Climate Change, edited by: Stocker, T. F., Qin, D., Plattner, G.-K., Tignor, M., Allen, S. K., Boschung, J., Nauels, A., Xia, Y., Bex, V., and Midgley, P. M.: Cambridge University Press, Cambridge, UK and New York, NY, USA, 2013. 4683

Cox, L. H. and March, R. S.: Comparison of geodetic and glaciological mass-balance techniques, Gulkana Glacier, Alaska, USA, J. Glaciol., 50, 363–370, doi:10.3189/172756504781829855, 2004. 4699

Crochet, P., Jóhannesson, T., Jónsson, T., Sigurðsson, O., Björnsson, H., Pálsson, F., and Barstad, I.: Estimating the spatial distribution of precipitation in Iceland using a linear model of orographic precipitation, J. Hydrometeorol., 2007. 4700

Cuffey, K. M. and Paterson, W. S. B.: The Physics of Glaciers, Elsevier, Burlington, 4th edn., 2010. 4693, 4702

Danish General Staff: Sheets: 87-NV,SV,SA, 97-NV, NA, 96-NA, Generalstabens Topografiske Afdeling, Copenhagen, 1904. 4688

Davies, B. J., Carrivick, J. L., Glasser, N. F., Hambrey, M. J., and Smellie, J. L.: Variable glacier response to atmospheric warming, northern Antarctic Peninsula, 1988–2009, The Cryosphere, 6, 1031–1048, doi:10.5194/tc-6-1031-2012, 2012. 4701

De Angelis, H.: Hypsometry and sensitivity of the mass balance to changes in equilibrium-line-altitude: the case of the Southern Patagonia Icefield, J. Glaciol., 60, 14–28, doi:10.3189/2014JoG13J127, 2014. 4698, 4701

De Woul, M., and Hock, R.: Static mass-balance sensitivity of Arctic glaciers and ice caps using a degree-day approach, Ann. Glaciol., 42, 217–224, doi:10.3189/172756405781813096, 2005. 4683

Defense Mapping Agency, H. C.: Series C761, sheets: 2113-I,2213-I,III,IV,2214-II,III, National LAnd Survey of Iceland, Reykjavík, 1997. 4688

Flowers, G. E. and Clarke, G. K. C.: Surface and bed topography of Trapridge Glacier, Yukon Territory, Canada: digital elevation models and derived hydraulic geometry, J. Glaciol., 45, 165–174, 1999. 4703

Flowers, G. E., Marshall, S. J., Björnsson, and Clarke, G. K. C.: Sensitivity of Vatnajökull ice cap hydrology and dynamics to climate warming over the next 2 centuries, J. Geophys. Res., 110, F02011, doi:10.1029/2004JF000200, 2005. 4684

Flowers, G. E., Björnsson, H., Geirsdóttir, A., Miller, G. H., and Clarke, G. K. C.: Glacier fluctuation and inferred climatology of Langjökull ice cap through the Little Ice Age, Quaternary Sci. Rev., 26, 2337–2353, 2007. 4683

Furbish, D. J. and Andrews, J. T.: The use of hypsometry to indicate long-term stability and response of valley glaciers to changes in mass transfer, J. Glaciol., 30, 199–211, 1984. 4693, 4698

Glasser, N. F., Harrison, S., Jansson, K. N., Anderson, K., and Cowley, A.: Global sea-level contribution from the Patagonian Icefields since the Little Ice Age maximum, Nat. Geosci., 4, 303–307, doi:10.1038/Ngeo1122, 2011. 4683

Guðmundsson, S.: Reconstruction of late 19th century glacier extent of Kotárjökull and Breiðamerkurjökull in SE–Iceland and comparison with the current extent, M.Sc. thesis, University of Iceland, Reykjavík, 2014. 4683, 4700

Guðmundsson, S., Pálsson, F., Björnsson, H., and Haraldsson, H. H.: Comparison of energy balance and degree-day models of summer ablation on the Langjökull ice cap, SW-Iceland, Jökull, 59, 1–18, 2009. 4699, 4700

Guðmundsson, S., Björnsson, H., Magnússon, E., Berthier, E., Pálsson, F., Guðmundsson, M. T., Högnadottir, T., and Dall, J.: Response of Eyjafjallajökull, Torfajökull and Tindfjallajökull ice caps in Iceland to regional warming, deduced by remote sensing, Polar Res., 30, doi:10.3402/Polar.V30i0.7282, 2011. 4692, 4694, 4699, 4700, 4733

Guðmundsson, S., Hannesdóttir, H., and Björnsson, H.: Post-Little Ice Age volume loss of Kotárjökull glacier, SE-Iceland, derived from historical photography, Jökull, 62, 97–110, 2012. 4688

Haeberli, W., Muller, P., Alean, P., and Bösch, H.: Glacier changes following the Little Ice Age-a survey of the international data basis and its perspectives, in: Glacier Fluctuations and Climatic Change, edited by: Oerlemans, J., Kluwer Academic Publishers, Utrecht, 1989. 4682

Hanna, E., Jonsson, T., and Box, J. E.: An analysis of icelandic climate since the nineteenth century, Int., 24, 1193–1210, 2004. 4700

Hannesdóttir, H., Björnsson, H., Pálsson, F., Aðalgeirsdóttir, G., and Guðmundsson, S.: Variations of southeast Vatnajökull ice cap (Iceland) 1650–1900 and reconstruction of the glacier surface geometry at the Little Ice Age maximum, Geografiska Annaler, in press. 4684, 4687, 4691, 4695, 4725, 4726, 4727, 4732, 4734

Huss, M.: Extrapolating glacier mass balance to the mountain-range scale: the European Alps 1900–2100, The Cryosphere, 6, 713–727, doi:10.5194/tc-6-713-2012, 2012. 4699, 4700

Huss, M.: Density assumptions for converting geodetic glacier volume change to mass change, The Cryosphere, 7, 877–887, doi:10.5194/tc-7-877-2013, 2013. 4694

Icelandic Meteorological Office and Institute of Earth Sciences, University of Iceland: DEMs of Icelandic glaciers (data set), The Icelandic Meteorological Office, Reykjavík, 2013. 4687

James, T. D., Murray, T., Barrand, N. E., Sykes, H. J., Fox, A. J., and King, M. A.: Observations of enhanced thinning in the upper reaches of Svalbard glaciers, The Cryosphere, 6, 1369–1381, doi:10.5194/tc-6-1369-2012, 2012. 4699

Jiskoot, H., Curran, C. J., Tessler, D. L., and Shenton, L. R.: Changes in Clemenceau Icefield and Chaba Group glaciers, Canada, related to hypsometry, tributary detachment, length-slope and area-aspect relations, Ann. Glaciol., 50, 133–143, 2009. 4693, 4701

Jóhannesson, T., Raymond, C., and Waddington, E.: Time-Scale for Adjustment of Glaciers to Changes in Mass Balance, J. Glaciol., 35, 355–369, 1989. 4702

Jóhannesson, T., Aðalgeirsdóttir, G., Björnsson, H., Crochet, P., Elíasson, E. B., Ólafsson, H., Pálsson, F., Rögnvaldsson, O., Sigurðsson, O., Snorrason, A., Blöndal Sveinsson, Ó. G., and Þorsteinsson, Þ: Effect of climate change on hydrology and hydro-resources in Iceland, Tech. Rep. OS-2007/011, Reykjavík, 2007. 4700

Jóhannesson, T., Björnsson, H., Pálsson, F., Sigurðsson, O., and Thorsteinsson, T.: LiDAR mapping of the Snæfellsjökull ice cap, western Iceland, Jökull, 61, 19–32, 2011. 4733

Jóhannesson, T., Björnsson, H., Magnússon, E., Guðmundsson, S., Pálsson, F., Sigurðsson, O., Thorsteinsson, T., and Berthier, E.: Ice-volume changes, bias estimation of mass-balance measurements and changes in subglacial lakes derived by lidar mapping of the surface of Icelandic glaciers, Ann. Glaciol., 54, 63–74, doi:10.3189/2013aog63a422, 2013. 4687, 4733

Jones, P. D., Lister, D. H., Osborn, T. J., Harpham, C., Salmon, M., and Morice, C. P.: Hemispheric and large-scale land surface air temperature variations: An extensive revision and an update to 2010, J. Geophys. Res., 35, L19502, doi:10.1029/2008GL034470, 2012. 4700

Kääb, A., and Funk, M.: Modelling mass balance using photogrammetric and geophysical data: a pilot study at Griesgletscher, Swiss Alps, J. Glaciol., 45, 575–583, 1999. 4689

Knoll, C., Kerschner, H., and Abermann, J.: Development of area, altitude and volume of South Tyrolean glaciers since the Little Ice Age maximum, Zeitschrift für Gletscherkunde und Glazialgeologie, 42, 19–36, 2008. 4683

Korona, J., Berthier, E., Bernard, M., Remy, F., and Thouvenot, E.: SPIRI T. SPOT 5 stereoscopic survey of Polar Ice: Reference Images and Topographies during the fourth International Polar Year (2007-2009), Int. Soc. Photogramme., 64, 204–212, doi:10.1016/j.isprsjprs.2008.10.005, 2009. 4689

Kuhn, M., Markel, G., Kaser, G., Nickus, U., Obleitner, F., and Schneider, H.: Fluctuations of climate and mass balances: different responses of two adjacent glaciers, Zeitschrift für Gletscherkunde und Glazialgeologie, 21, 409–416, 1985. 4701

Lliboutry, L.: Nieves y Glaciares de Chile: Fundamentos de glaciología, University of Chile, Santiago, 1956. 4693

Luthcke, S. B., Arendt, A. A., Rowlands, D. D., McCarthy, J. J., and Larsen, C. F.: Recent glacier mass changes in the Gulf of Alaska region from GRACE mascon solutions, J. Glaciol., 54, 767–777, doi:10.3189/002214308787779933, 2008. 4699

Lüthi, M. P., Bauder, A., and Funk, M.: Volume change reconstruction of Swiss glaciers from length change data, J. Geophys. Res.-Earth, 115, F04022, doi:10.1029/2010jf001695, 2010. 4683

Magnússon, E., Björnsson, H., and Pálsson, F.: Landslag í grennd Kvískerja í fortíð og framtíð: Niðurstöður ísjármælinga á Kvíár-, Hrútár og Fjallsjökli (Radio echo sounding on Kvíárjökull, Hútárjökull and Fjallsjökull)., Jökull, 57, 83–89, 2007. 4689

Magnússon, E., Pálsson, F., Björnsson, H., and Guðmundsson, S.: Removing the ice cap of Öraefajokull central volcano, SE-Iceland: Mapping and interpretation of bedrock topography, ice volumes, subglacial troughs and implications for hazards assessments, Jökull, 62, 131–150, 2012. 4685, 4689

Marshall, S. J.: Modelling glacier response to climate change, in: Glacier Science and Environmental Change, edited by: Knight, P. G., Blackwell Publishing, Malden, USA, 275–292, 2008. 4693

Mathieu, R., Chinn, T., and Fitzharris, B.: Detecting the equilibrium-line altitudes of New Zealand glaciers using ASTER satellite images, New Zealand J. Geol. Geophys., 52, 209–222, 2009. 4693

Mernild, S. H., Pelto, M., Malmros, J. K., Yde, J. C., Knudsen, N. T., and Hanna, E.: Identification of snow ablation rate, ELA, AAR and net mass balance using transient snowline variations on two Arctic glaciers, J. Glaciol., 59, 649–659, doi:10.3189/2013jog12j221, 2013. 4693

Möller, M., and Schneider, C.: Calibration of glacier volume-area relations from surface extent fluctuations and application to future glacier change, J. Glaciol., 56, 33–40, 2010. 4703

Nawri, N., and Björnsson, H.: Surface Air Temperature and Precipitation Trends for Iceland in the 21st Century, Tech. Rep. VÍ 2010-005, The Icelandic Meteorological Office, Reykjavík, 2010.

Oerlemans, J.: Estimating the reponse times of Vadret da Morteratsch, Vadret da Palu, Briksdalsbreen and Nigardsbreen from their length records, J. Glaciol., 53, 357–362, 2007. 4701, 4703

Oerlemans, J., Anderson, B., Hubbard, A., Huybrechts, P., Johannesson, T., Knap, W. H., Schmeits, M., Stroeven, A. P., van de Wal, R. S. W., Wallinga, J., and Zuo, Z.: Modelling the response of glaciers to climate warming, Clim. Dynam., 14, 267–274, 1998. 4693, 4701

Osmaston, H. A.: Models for the estimation of firnlines of present and Pleistocene glaciers, in: Processes in physical and human geography: Bristol essays, edited by: PeeL, R. F., Chisholm, M. D. I., and Haggart, P., 218–245, Heinemann Educational Books Ltd, London, 1975. 4698

Östrem, G.: ERTS data in glaciology- an effort to monitor glacier mass balance from satellite imagery, J. Glaciol., 15, 403–415, 1975. 4693

Pálsson, F., Guðmundsson, S., Björnsson, H., Berthier, E., Magnússon, E., Guðmundsson, S., and Haraldsson, H. H.: Mass and volume changes of Langjokull ice cap, Iceland, similar to ∼1890 to 2009, deduced from old maps, satellite images and in situ mass balance measurements, Jökull, 62, 81–96, 2012. 4683, 4688, 4692, 4694, 4699, 4700, 4733

Paul, F., Kääb, A., Maisch, M., Kellenberger, T., and Haeberli, W.: Rapid disintegration of Alpine glaciers observed with satellite data, Geophys. Res. Lett., 31, doi:10.1029/2004gl020816, 2004. 4699

Paul, F., Kääb, A., and Haeberli, W.: Recent glacier changes in the Alps observed by satellite: Consequences for future monitoring strategies, Global Planet. Change, 56, 111–122, doi:10.1016/j.gloplacha.2006.07.007, 2007. 4690

Pelto, M. S.: Forecasting temperate alpine glacier survival from accumulation zone observations, The Cryosphere, 4, 67–75, doi:10.5194/tc-4-67-2010, 2010. 4690, 4699

Rabatel, A., Machaca, A., Francou, B., and Jomelli, V.: Glacier recession on Cerro Charquini (16 degrees S), Bolivia, since the maximum of the Little Ice Age (17th century), J. Glaciol., 52, 110–118, doi:10.3189/172756506781828917, 2006. 4683

Rabatel, A., Francou, B., Soruco, A., Gomez, J., Cáceres, B., Ceballos, J. L., Basantes, R., Vuille, M., Sicart, J.-E., Huggel, C., Scheel, M., Lejeune, Y., Arnaud, Y., Collet, M., Condom, T., Consoli, G., Favier, V., Jomelli, V., Galarraga, R., Ginot, P., Maisincho, L., Mendoza, J., Ménégoz, M., Ramirez, E., Ribstein, P., Suarez, W., Villacis, M., and Wagnon, P.: Current state of glaciers in the tropical Andes: a multi-century perspective on glacier evolution and climate change, The Cryosphere, 7, 81–102, doi:10.5194/tc-7-81-2013, 2013. 4693

Radic, V., Hock, R., and Oerlemans, J.: Volume-area scaling vs flowline modelling in glacier volume projections, Ann. Glaciol., 46, 234–240, 2007. 4703, 4704

Reinhardt, W. and Rentsch, H.: Determination of chnages in volume and elevation of glaciers using digital elevation models for the Veragtferner, Ötztal Alps, Austria, Ann. Glaciol., 8, 151–155, 1986. 4689

Rivera, A., Benham, T., Casassa, G., Bamber, J., and Dowdeswell, J. A.: Ice elevation and areal changes of glaciers from the Northern Patagonia Icefield, Chile, Global Planet. Change, 59, 126–137, doi:10.1016/j.gloplacha.2006.11.037, 2007. 4690

Rögnvaldsson, O., Jónsdóttir, J. F., and Ólafsson, H.: Numerical simulations of precipitation in the complex terrain of Iceland- Comparison with glaciological and hydrological data, Meterol. Z., 16, 71–85, 2007. 4700

Shea, J. M., Menounos, B., Moore, R. D., and Tennant, C.: An approach to derive regional snow lines and glacier mass change from MODIS imagery, western North America, The Cryosphere, 7, 667–680, doi:10.5194/tc-7-667-2013, 2013. 4693

Sigurðsson, F.: Vandamál við úrkomumælingar á Íslandi, in: Vatnið og landið. Vatnafræðiráðstefna, Október 1987, edited by: Sigbjarnarson, G., Orkustofnun, Reykjavík, 307, 101–110, 1990. 4687

Thórarinsson, S.: Oscillations of the Iceland glaciers in the last 250 years, Geogr. Ann. A, 25, 1–54, 1943. 4684, 4703

Vaughan, D. G., Comiso, J. C., Allison, I., Carrasco, J., Kaser, G., Kwok, R., Mote, P., Murray, T., Paul, F., Ren, J., Rignot, E., Solomina, O., Steffen, K., and Zhang, T.: Observations: Cryosphere, in: Climate Change 2013: The Physical Science Basis. Contribution of Working Group I to the Fifth Assessment Report of the Intergovernmental Panel on Climate Change, edited by: Stocker, T. F., Qin, D., Plattner, G.-K., Tignor, M., Allen, S. K., Boschung, J., Nauels, A., Xia, Y., Bex, V., and Midgley, P. M.: Cambridge University Press, Cambridge, UK and New York, NY, USA, 317–382, 2013. 4682, 4699, 4703, 4705

WGMS: Global Glacier Changes: Facts and Figures, Tech. rep., Zurich, Switzerland, 2008. 4682

Wise, S.: Assessing the quality for hydrological applications of digital elevation models derived from contours, Hydrol. Process., 14, 1909–1929, doi:10.1002/1099-1085(20000815/30)14:11/12<1909::Aid-Hyp45>3.0.Co;2-6, 2000. 4690

TCD

8, 4681–4735, 2014

Table 1. Characteristics of the southeast outlet glaciers. Some glaciers have gently sloping accumulation and ablation areas, which are connected by ice falls, thus the mean slope is not representative for the entire profile. The ELA is presented as the range of the averages of all years. Average ice thickness and terminus elevation are presented in ~ 1890 and 2010.

glacier	slope (°)	ice divide (m a.s.l.)	area (km^2)	volume (km^3)	thickness (m)	AAR	ELA (m a.s.l.)	length (km)	term. elev. (m a.s.l.)	retreat (km)	hypsom.
Morsárj.	6.3	1350	28.9	6.0	215/208	0.64	1000–1130	10.8	150/170	1.8	B
Skaftafellsj.	3.8	1880	84.1	20.3	254/241	0.66	1000–1160	19.3	80/95	2.5	B
Svínafellsj.	9.0	2030	33.2	3.6	132/108	0.66	1000–1120	12.0	90/100	0.8	E
Kotárj.	13.3	1820	11.5	1.7	152/148	0.71	1000–1130	6.2	220/400	1.3	B/D
Kvíárj.	6.0	2010	23.2	4.1	187/177	0.64	1010–1130	14.1	30/30	1.5	E
Hrútárj.	12.4	1980	12.2	0.9	111/74	0.58	880–910	8.6	50/60	2.0	A/C
Fjallsj.	7.9	2030	44.6	7.0	185/157	0.6	870–960	12.9	20/30	2.2	E/C
Skálafellsj.	3.1	1490	100.6	33.3	332/331	0.68	910–1020	24.4	40/50	2.0	B
Heinabergsj.	3.7	1490	99.7	26.7	308/268	0.61	990–1100	22.7	60/70	2.9	B/C
Fláaj.	3.1	1480	169.8	53.9	313/317	0.59	1060–1120	25.1	40/70	2.7	B
Hoffellsj.	3.4	1470	206.0	54.3	303/264	0.63	1050–1120	23.6	30/50	4.0*	B/D
Lambatungnaj.	5.0	1480	36.3	3.6	135/99	0.43	1110–1210	19.3	180/250	2.7	D

*The retreat applies to the western arm of Hoffellsjökull (named Svínafellsjökull).

Table 2. Area of the outlet glaciers at different times in km^2. The estimated error of the glacier margin is shown in parenthesis in the top row. The DMA aerial photographs of Öræfajökull are from 1982, and of the eastern outlet glaciers from 1989. Glacier outlines from 2002 for Öræfajökull (obtained from images of Loftmyndir ehf.), and from 2000 for Skálafellsjökull, Heinabergsjökull, Fláajökull, Hoffellsjökull and Lambatungnajökull (digitized from Landsat satellite images). Ice divides are assumed to remain constant throughout the time period. The numbers for Hoffellsjökull are from Aðalgeirsdóttir et al. (2011). Percentages are relative to the ~ 1890 area. *The area of Lambatungnajökull in 1904 is estimated from the relative extent of the neighbouring outlets in that year (99 %). Kotárjökull is not included in the sum of the Öræfajökull outlets, since its area is only known in ~ 1890 and 2010.

glacier	~ 1890 (20 m)	1904 (15 m)	1945 (10 m)	1982/1989 (10 m)	2002 (5 m)	2010 (2 m)
Morsárj.	35.3 ± 0.7	34.5 ± 0.6 (98 %)	31.6 ± 0.3 (90 %)	30.9 ± 0.4 (87 %)	30.0 ± 0.2 (85 %)	28.9 ± 0.1 (82 %)
Skaftafellsj.	97.8 ± 1.3	96.7 ± 1.0 (99 %)	90.1 ± 0.6(92 %)	89.4 ± 0.6 (91 %)	86.4 ± 0.3 (88 %)	84.1 ± 0.1 (86 %)
Svínafellsj.	39.5 ± 0.9	38.9 ± 0.7 (98 %)	36.1 ± 0.5 (91 %)	35.5 ± 0.5 (90 %)	34.8 ± 0.3 (88 %)	33.2 ± 0.1 (84 %)
Kotárj.	14.5 ± 0.4		12.3 ± 0.5 (85 %)			11.5 ± 0.04 (79 %)
Kvíárj.	27.9 ± 0.7	27.4 ± 0.5 (98 %)	25.4 ± 0.4 (91 %)	25.1 ± 0.3 (90 %)	24.4 ± 0.2 (88 %)	23.2 ± 0.1 (83 %)
Hrútárj.	17.1 ± 0.5	16.7 ± 0.4 (98 %)	14.1 ± 0.2 (83 %)	13.9 ± 0.2 (81 %)	13.2 ± 0.1 (77 %)	12.2 ± 0.04 (71 %)
Fjallsj.	57.7 ± 0.8	56.1 ± 0.6 (97 %)	51.7 ± 0.4 90 %)	49.4 ± 0.4 (86 %)	47.3 ± 0.2 (82 %)	44.6 ± 0.1 (77 %)
Öræfaj.	275.3 ± 5.3	270.3 ± 3.8	249.0 ± 2.4	244.1 ± 2.4	236.1 ± 1.3	181.6 ± 0.58
Skálafellsj.	117.9 ± 1.6	116.4 ± 1.2 (99 %)	106.6 ± 0.7 (90 %)	104.0 ± 0.7 (88 %)	102.8 ± 0.3 (87 %)	100.6 ± 0.1 (85 %)
Heinabergsj.	120.3 ± 1.3	118.2 ± 1.0 (98 %)	109.0 ± 0.6 (91 %)	102.5 ± 0.6 (85 %)	101.8 ± 0.3 (85 %)	100.6 ± 0.1 (83 %)
Fláaj.	205.6 ± 1.9	202.1 ± 1.4 (98 %)	184.1 ± 1.0 (90 %)	181.9 ± 0.9 (88 %)	177.4 ± 0.5 (86 %)	169.7 ± 0.2 (83 %)
Hoffellsj.	234.5 ± 1.9	232.3 ± 1.4 (99 %)	224.5 ± 1.1 (96 %)	215.9 ± 1.0 (92 %)	212.7 ± 0.5 (91 %)	207.5 ± 0.2 (88 %)
Lambatungnaj.	46.1 ± 0.9	45.1 ± 0.9*	40.9 ± 0.4 (89 %)	39.4 ± 0.4 (86 %)	38.8 ± 0.2 (84 %)	36.3 ± 0.1 (79 %)
Eastern	723.9 ± 7.6	714.2 ± 5.9	664.6 ± 3.8	643.8 ± 3.6	632.8 ± 1.8	612.3 ± 0.7

1936 area: Hoffellsjökull 227.7 ± 1.5 (97%), Lambatungnajökull 41.9 ± 0.7 (91%).

TCD
8, 4681–4735, 2014

Area, volume and mass changes of southeast Vatnajökull ice cap

Hannesdóttir et al.

Title Page
Abstract | Introduction
Conclusions | References
Tables | Figures
◂◂ | ▸▸
◂ | ▸
Back | Close
Full Screen / Esc
Printer-friendly Version
Interactive Discussion

Table 3. Volume of the southeast outlet glaciers derived from glacier surface DEMs and the bedrock DEM at different times in km^3. Percentage is relative to the ~ 1890 volume. The estimated point accuracy of the elevation is in parenthesis. * The volume of Lambatungnajökull in 1904 is estimated from the relative size of the neighbouring outlets in that year (99%). Kotárjökull is not included in the sum of the Öræfajökull outlets, since its volume is only known in ~ 1890 and 2010.

glacier	~ 1890 (15–20 m)	1904 (10–15 m)	1945 (5–10 m)	1989 (5 m)	2002 (2 m)	2010 (0.5 m)
Morsárj.	7.6 ± 0.5	7.5 ± 0.4 (99 %)	6.8 ± 0.2 (89 %)		6.3 ± 0.1 (82 %)	6 ± 0.01 (79 %)
Skaftafellsj.	24.8 ± 1.5	24.5 ± 1.0 (99 %)	21.4 ± 0.6 (86 %)		20.7 ± 0.2 (83 %)	19.9 ± 0.04 (80 %)
Svínafellsj.	5.2 ± 0.6	5.1 ± 0.4 (99 %)	4.4 ± 0.3 (84 %)		4.1 ± 0.1 (78 %)	3.6 ± 0.02 (70 %)
Kotárjökull	2.2 ± 0.2					1.7 ± 0.01 (77 %)
Kvíárjökull	5.2 ± 0.4	5.15 ± 0.3 (99 %)	4.5 ± 0.2 (87 %)		4.2 ± 0.05 (81 %)	4.1 ± 0.01 (79 %)
Hrútárjökull	1.9 ± 0.3	1.8 ± 0.2 (96 %)	1.3 ± 0.1 (68 %)		1.08 ± 0.03 (57 %)	0.93 ± 0.01 (49 %)
Fjallsjökull	10.7 ± 0.9	10.3 ± 0.6 (97 %)	8.9 ± 0.4 (83 %)		7.3 ± 0.1 (69 %)	7 ± 0.02 (65 %)
Öræfajökull	55.4 ± 4.4	54.5 ± 2.9	47.2 ± 1.8		43.5 ± 0.58	41.3 ± 0.12
Skálafellsj.	39.1 ± 1.8	38.7 ± 1.2 (99 %)	35.7 ± 0.8 (91 %)	34.9 ± 0.5 (89 %)	34.6 ± 0.2 (88 %)	33.3 ± 0.05 (85 %)
Heinabergsj.	37 ± 1.8	36.6 ± 1.2 (99 %)	32.4 ± 0.8 (88 %)	29.4 ± 0.5 (80 %)	29.1 ± 0.2 (79 %)	26.7 ± 0.05 (72 %)
Fláajökull	64.3 ± 3.1	63.4 ± 2.0 (99 %)	57.7 ± 1.3 (90 %)	57.2 ± 0.9 (89 %)	56.2 ± 0.4 (87 %)	53.9 ± 0.09 (84 %)
Hoffellsj.	71 ± 4	70.4 ± 2.3 (99 %)	63 ± 2 (89 %)	57.6 ± 1.1 (81 %)	57 ± 0.4 (80 %)	54.3 ± 0.1 (76 %)
Lambatungnaj.	6.2 ± 0.7	6.1 ± 0.7 (99 %)	4.7 ± 0.3 (76 %)	4.4 ± 0.2 (76 %)	4.1 ± 0.1 (66 %)	3.6 ± 0.02(58 %)
Eastern outlets	217.6 ± 11.4	215.2 ± 7.4	193.5 ± 5.2	183.6 ± 3.2	180.9 ± 1.3	171.8 ± 0.31

1936 volume: Hoffellsjökull 65 ± 3 (92%), Lambatungnajökull 4.9 ± 0.4 (79%).

Table 4. Geodetic mass balance in m w.e. a^{-1} for outlets of Öræfajökull (upper panel) and the eastern outlet glaciers (lower panel) for different time intervals. The correlation of the average summer (JJA) temperature measured at Hólar in Hornafjörður (shown as ave. T) with geodetic mass balance estimates during the same time intervals is shown in the last column.

Öræfaj.	~ 1890–1904	1904–1945	1945–2002	2002–2010	~ 1890–2010	corr. T (r)
Morsárj.	−0.18 ± 0.63	−0.48 ± 0.15	−0.26 ± 0.06	−0.99 ± 0.12	−0.37 ± 0.96	0.98
Skaftaf.	−0.19 ± 0.63	−0.73 ± 0.15	−0.13 ± 0.06	−1.06 ± 0.12	−0.40 ± 0.96	0.94
Svínaf.	−0.1 ± 0.63	−0.46 ± 0.15	−0.2 ± 0.06	−0.89 ± 0.12	−0.32 ± 0.96	0.98
Kvíárj.	−0.12 ± 0.63	−0.54 ± 0.15	−0.17 ± 0.06	−0.8 ± 0.12	−0.34 ± 0.96	0.96
Hrútárj.	−0.27 ± 0.63	−0.77 ± 0.15	−0.24 ± 0.06	−1.33 ± 0.12	−0.5 ± 0.96	0.96
Fjallsj.	−0.41 ± 0.63	−0.6 ± 0.15	−0.48 ± 0.06	−1-.27 ± 0.12	−0.57 ± 0.96	0.96
ave. T	9.2	9.9	9.7	10.6		

Eastern	~ 1890–1904	1904–1945	1936–1945	1945–1989	1989–2002	2002–2010	~ 1890–2010	corr. T (r)
Skálaf.	−0.24 ± 0.63	−0.58 ± 0.15		−0.27 ± 0.08	−0.25 ± 0.19	−1.38 ± 0.12	−0.40 ± 0.96	0.96
Heinab.	−0.22 ± 0.63	−0.81 ± 0.15		−0.56 ± 0.08	−0.36 ± 0.19	−2.6 ± 0.12	−0.70 ± 0.96	0.97
Fláaj.	−0.28 ± 0.63	−0.65 ± 0.15		−0.42 ± 0.08	−0.4 ± 0.19	−1.51 ± 0.12	−0.42 ± 0.96	0.97
Hoff.	−0.16 ± 0.63	−0.71 ± 0.15	−0.88 ± 0.39	−0.46 ± 0.08	−0.35 ± 0.19	−1.45 ± 0.12	−0.57 ± 0.96	0.94
Lambat.	−0.14 ± 0.63	−0.6 ± 0.15	−0.68 ± 0.39	−0.17 ± 0.08	−0.48 ± 0.19	−1.5 ± 0.12	−0.47 ± 0.96	0.94
ave. T	9.2	9.9	10.4	9.7	9.7	10.6		

1904–1936 mb: Hoffellsjökull −0.66 ± 0.39, Lambatungnajökull −0.51 ± 0.39.

TCD

8, 4681–4735, 2014

Area, volume and mass changes of southeast Vatnajökull ice cap

Hannesdóttir et al.

Table 5. The scaling exponent γ and coefficient c derived from the best fit line of every year.

year	γ	c
all	1.405	0.038
1890	1.357	0.048
1904	1.387	0.043
1945	1.430	0.034
2002	1.457	0.030
2010	1.391	0.040

TCD
8, 4681–4735, 2014

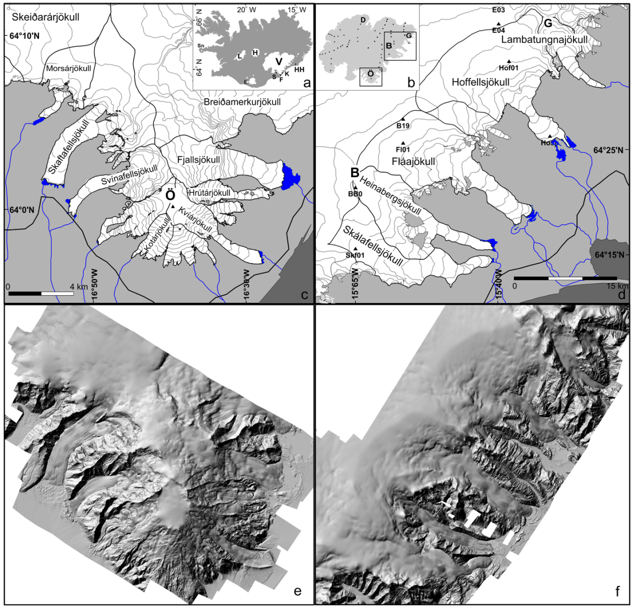

Figure 1. (a) Iceland and Vatnajökull (V) and other ice caps and glaciers mentioned in the text, Hofsjökull (H), Langjökull (L), Eyjafjallajökull (E), and Snæfellsjökull (Sn). Weather stations in Skaftafell (S), Fagurhólsmýri (F), Kvísker (K) and Hólar in Hornafjörður (HH). **(b)** Vatnajökull and mass balance stakes (black dots), the insets show the outline of figures **(c)** the outlet glaciers descending from Öræfajökull ice cap (Ö) and Morsárjökull and **(d)** the outlet glaciers east of Breiðamerkurjökull, descending from the Breiðabunga dome (B), and Goðahnúkar (G), D = Dyngjujökull (mentioned later in the text). The surface topography is from the 2010 LiDAR DEMs, with 100 m contour lines, and ice divides are delineated in black. The location of mass balance measurements is indicated with triangles. Note the different scale of the two figures. Proglacial lakes and rivers are shown in blue and highway 1 in black. (**e** and **f**) Topographic relief shading of the LiDAR DEMs of the same area as in **(a)** and **(b)**. The LIA terminal moraines are clearly visible in front of the glaciers and a number of ice-marginal lakes.

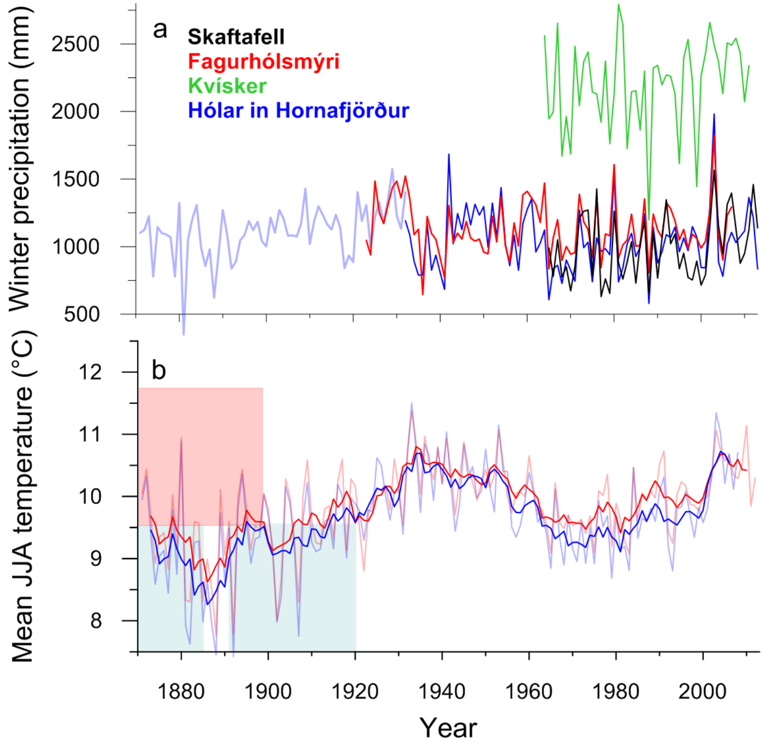

Figure 2. (a) Winter precipitation (October–April in mm) at Skaftafell (black), Fagurhólsmýri (red), Kvísker (green) and Hólar in Hornafjörður (blue), see Fig. 1a for location of stations. Reconstructed precipitation indicated with a light blue line (from Aðalgeirsdóttir et al., 2011). **(b)** Mean summer (JJA) temperature at Fagurhólsmýri (red) and Höfn in Hornafjörður (blue) and 5 years running average. Light blue and light red boxes indicate time period of reconstructed temperature (from Aðalgeirsdóttir et al., 2011).

TCD
8, 4681–4735, 2014

Title Page
Abstract Introduction
Conclusions References
Tables Figures
◂I ▸I
◂ ▸
Back Close
Full Screen / Esc
Printer-friendly Version
Interactive Discussion

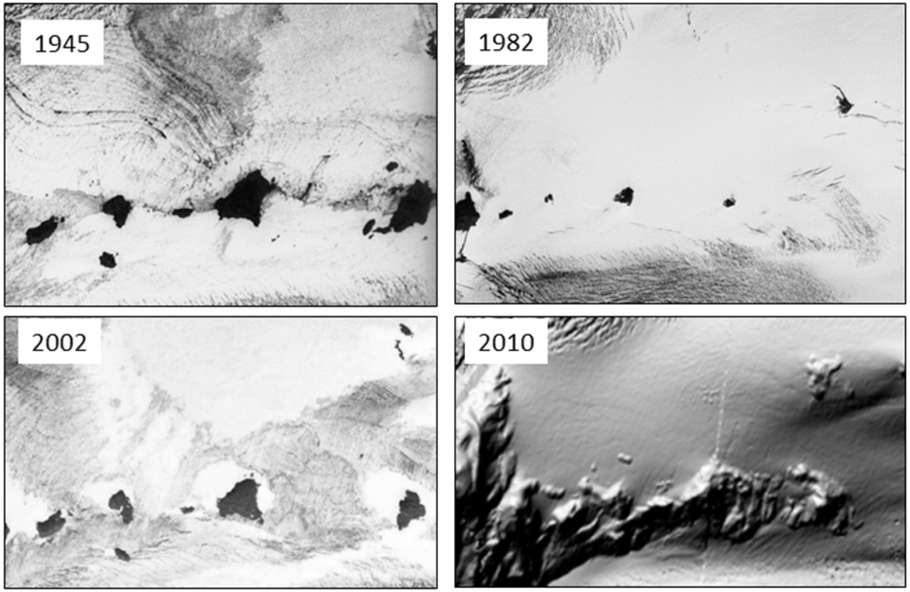

Figure 3. Small nunataks at an elevation of 950–1050 m, east of the mountain "Skerið milli skarða", which divides the main branch of Skaftafellsjökull (see Fig. 5), at different times. Aerial photograph of National Land Survey of Iceland 1945 and 1982, aerial image of Loftmyndir ehf. from 2002, LiDAR shaded relief map from 2010. Only the largest mid nuntak is visible on the 1904 map (not shown).

TCD
8, 4681–4735, 2014

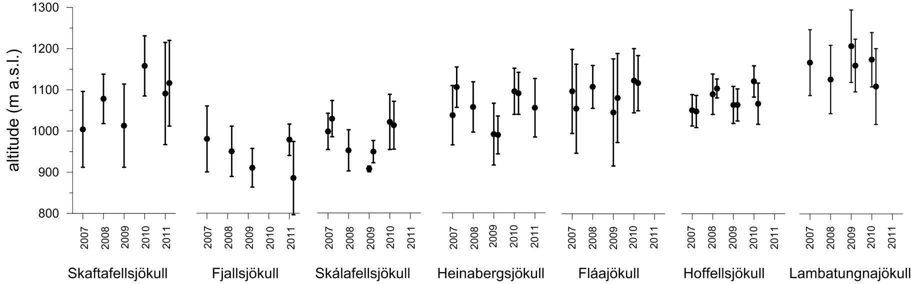

Figure 4. The elevation range (average and standard deviation) of the snowline for each glacier deduced from MODIS images (2007–2011); the elevation obtained from the LiDAR DEM.

TCD
8, 4681–4735, 2014

Area, volume and mass changes of southeast Vatnajökull ice cap

Hannesdóttir et al.

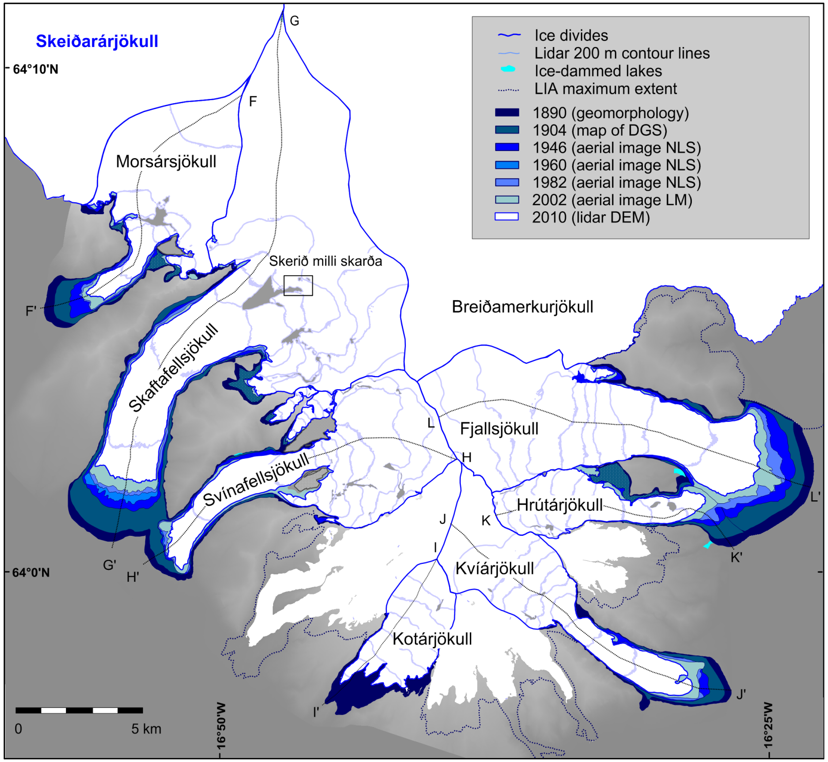

Figure 5. The extent of Öræfajökull's outlet glaciers and Morsárjökull at different times. The surface map is derived from the LiDAR DEM, showing 200 m contour lines. The locations of longitudinal profiles shown in Fig. 8 are indicated with capital letters F-F′, G-G′, etc. The area covering the nunataks east of "Skerið milli skarða", shown in Fig. 3 is outlined. The ice extent in 1904 is uncertain in the mountains surrounding Morsárjökull and Skaftafellsjökull, due to distorted topography on the old map. DGS = Danish General Staff, NLS = National Land Survey of Iceland, LM = Loftmyndir ehf. The ~ 1890 glacier extent is from Hannesdóttir et al. (2014).

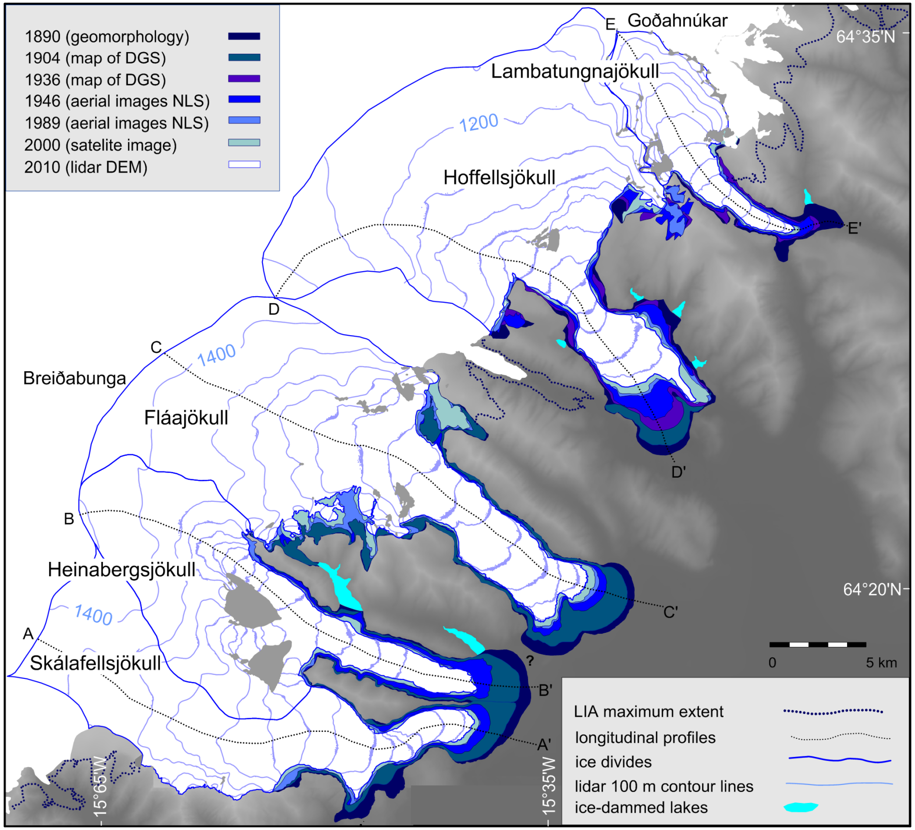

Figure 6. The extent of Skálafellsjökull, Heinabergsjökull, Fláajökull, Hoffellsjökull and Lambatungnajökull at different times. The locations of longitudinal profiles shown in Fig. 8 are indicated with capital letters (A-A′, B-B′ etc.). Surface map is derived from the LiDAR DEM, showing 100 m contour lines. (DGS = Danish General Staff, NLS = National Land Survey of Iceland). The ~ 1890 glacier extent is from Hannesdóttir et al. (2014).

TCD
8, 4681–4735, 2014

Area, volume and mass changes of southeast Vatnajökull ice cap

Hannesdóttir et al.

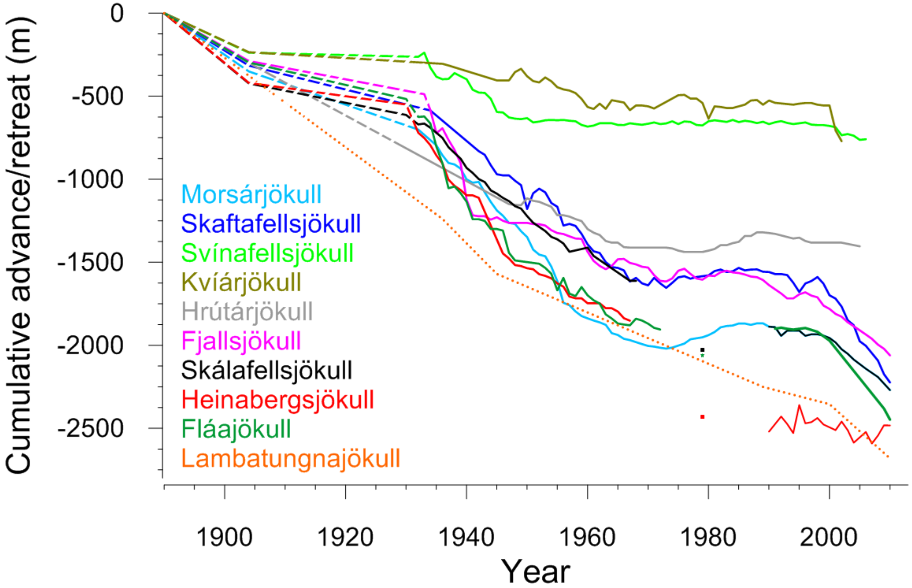

Figure 7. Cumulative frontal variations of the southeast outlet glaciers relative to the ∼ 1890 terminus position determined from the terminal LIA moraines (Hannesdóttir et al., 2014). The retreat until 1932, when measurements of volunteers of the Icelandic Glaciological Society started, is indicated by broken lines; the position in 1904 is known from the maps of the Danish General Staff; note that a linear recession is not expected in ∼ 1890–1904 or 1904–1932. Annual measurements are shown with an unbroken line (http://spordakost.jorfi.is). Skálafellsjökull, Heinabergsjökull and Fláajökull were not measured in the 1970s and 1980s, but their terminus position in 1979 is determined from aerial images of the National Land Survey of Iceland (indicated by dots). The terminus of Lambatungnajökull (dotted line) has not been measured, but its recession is retrieved from maps, aerial photographs and satellite images.

TCD
8, 4681–4735, 2014

Area, volume and mass changes of southeast Vatnajökull ice cap

Hannesdóttir et al.

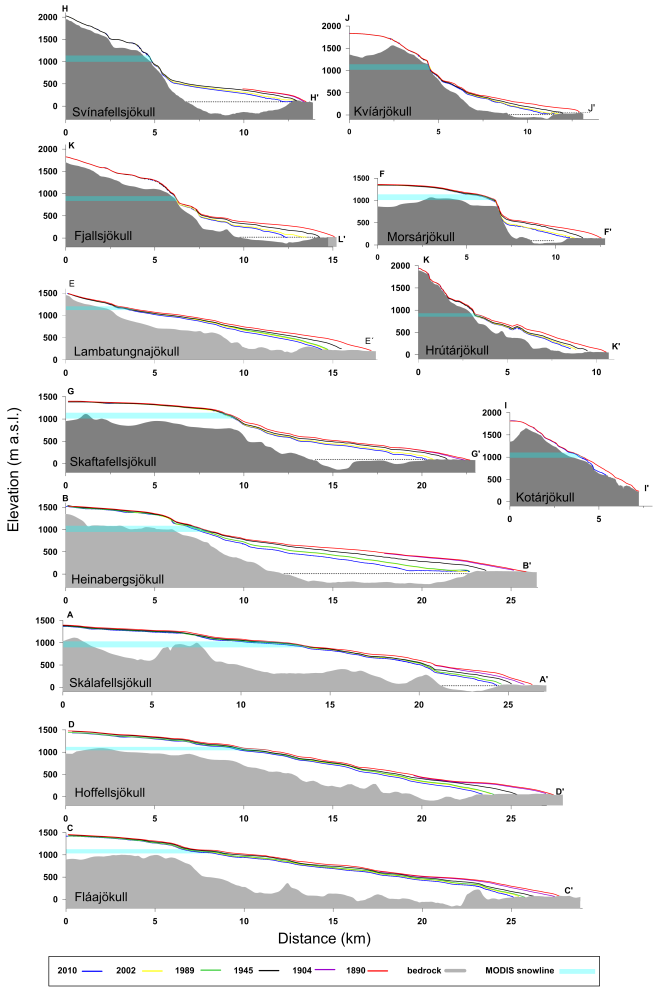

TCD
8, 4681–4735, 2014

Title Page
Abstract | Introduction
Conclusions | References
Tables | Figures
◀◀ | ▶▶
◀ | ▶
Back | Close
Full Screen / Esc
Printer-friendly Version
Interactive Discussion

Figure 8. Longitudinal profiles of the southeast outlet glaciers, showing ice thickness and location of the termini at different times. The average ELA derived from the MODIS images is shown with a light blue horizontal line. Öræfajökull outlets with dark gray colored bedrock and the eastern outlets with light gray colored bedrock.

TCD
8, 4681–4735, 2014

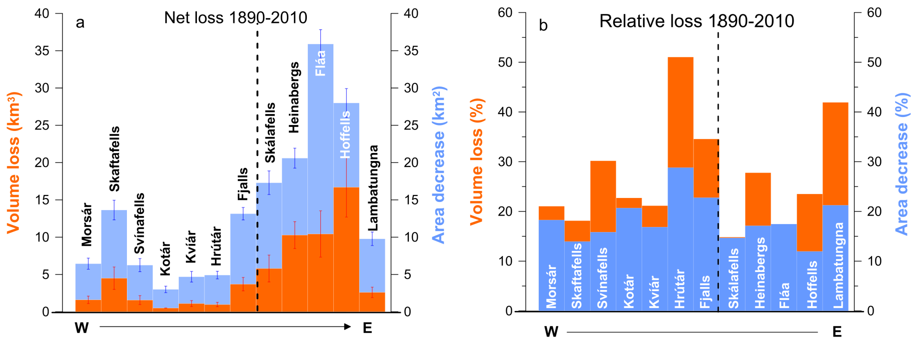

Figure 9. Total area decrease (light blue) and volume loss (orange) during the time period ~1890–2010 **(a)** absolute values, and **(b)** relative to the LIA maximum size. Glaciers represented in geographical order and the dotted line separates the outlets of Öræfajökull and the eastern outlets.

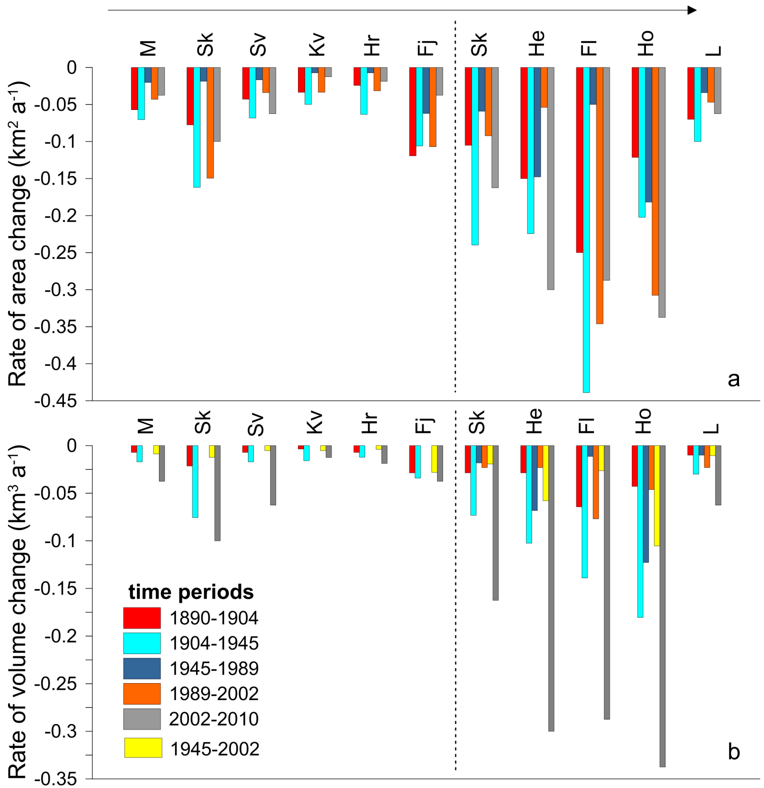

Figure 10. Rate of area **(a)** and volume **(b)** change of the outlet glaciers (from west to east) during different time periods of the last 120 years. The first few letters of each glacier name are shown at the top, glaciers represented in geographical order, from west to east. The dotted line separates the outlets of Öræfajökull and the eastern outlets.

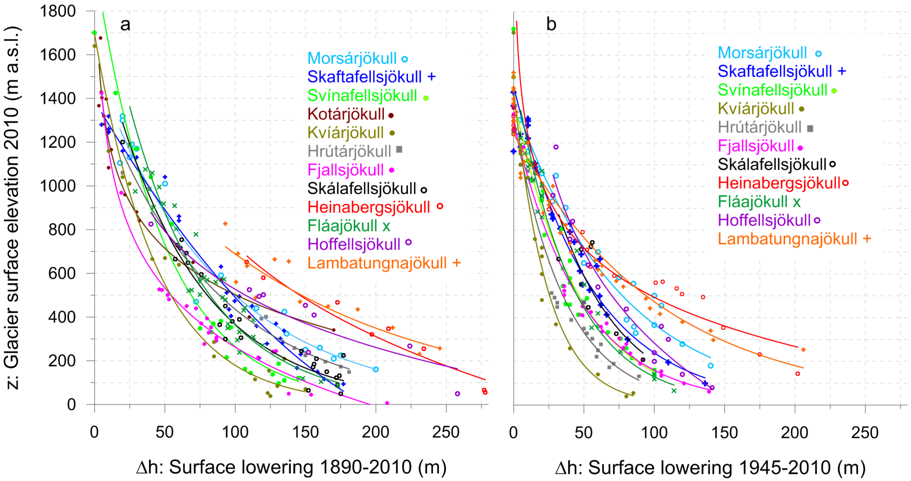

Figure 11. Average surface lowering of every 20 m altitudinal interval of the outlets of southeast Vatnajökull. **(a)** Between ~ 1890 and 2010 (modified from Hannesdóttir et al., 2014). The ~ 1890 glacier surface elevation in the accumulation area is derived from historical photographs, survey elevation points on the 1904 maps and the aerial images of Loftmyndir ehf., and in the ablation area it is mainly deduced from glacial geomorphological features. **(b)** Between 1945 and 2010. The glacier surface lowering in the accumulation area is based on comparison of the size of nunataks as observed on the original aerial images of 1945 and the LiDAR DEMs. No 1945 DEM is available for Kotárjökull.

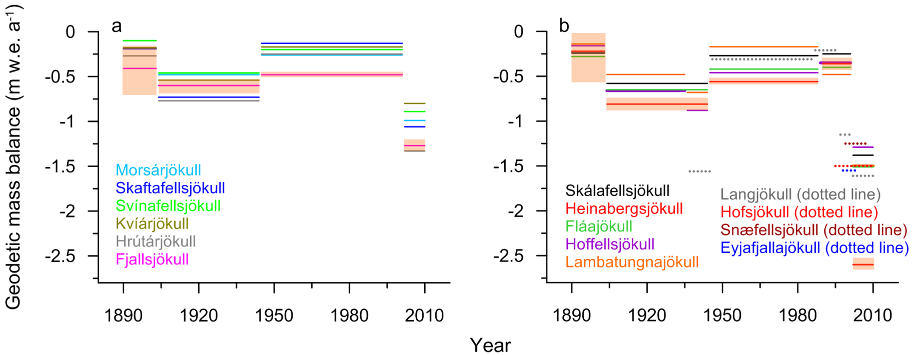

Figure 12. Geodetic mass balance rates during different time periods of the last 120 years. **(a)** The outlet glaciers of Öræfajökull and Morsárjökull. **(b)** The eastern outlet glaciers. For comparison, the geodetic mass balance of Langjökull (Pálsson et al., 2012), Eyjafjallajökull 1998–2004 (Guðmundsson et al., 2011), Snæfellsjökull 1999–2008 (Jóhannesson et al., 2011), and Hofsjökull 1995–2010 (Jóhannesson et al., 2013) is presented with dotted lines in **(b)**. The two latest time periods of Langjökull (1997–2002 and 2002–2010) are based on surface mass balance measurements (data base Glaciological group Institute of Earth Sciences, University of Iceland). For error estimates of the geodetic mass balance see Table 4, only the error bars for Fjallsjökull and Heinabergsjökull are shown here.

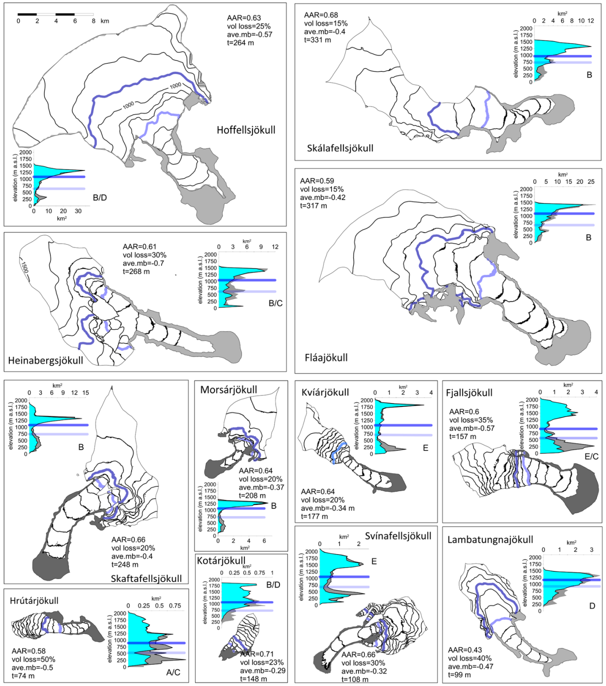

Figure 13. The topography of the outlet glaciers in 2010 with 100 m contour lines of the LiDAR DEM. The ∼ 1890 areal extent is shown in dark gray for the Öræfajökull outlets and in light gray for the eastern outlets. The average MODIS-derived ELA (2007–2011) is drawn in dark blue on the map, and the inferred ELA of the maximum LIA in light blue (Hannesdóttir et al., 2014). Inset graphs show the 2010 area-altitude distribution of the glaciers (hypsometry) in 2010 (cyan) and ∼ 1890 (gray), with the average ELA for 2010 and ∼ 1890 shown in dark blue and light blue, respectively. The AAR, the relative volume loss of their ∼ 1890 size, the average geodetic mass balance ∼1890–2010 is shown in m w.e. a^{-1}, as well as the average ice thickness (t) in 2010, for every glacier.

TCD

8, 4681–4735, 2014

Area, volume and mass changes of southeast Vatnajökull ice cap

Hannesdóttir et al.

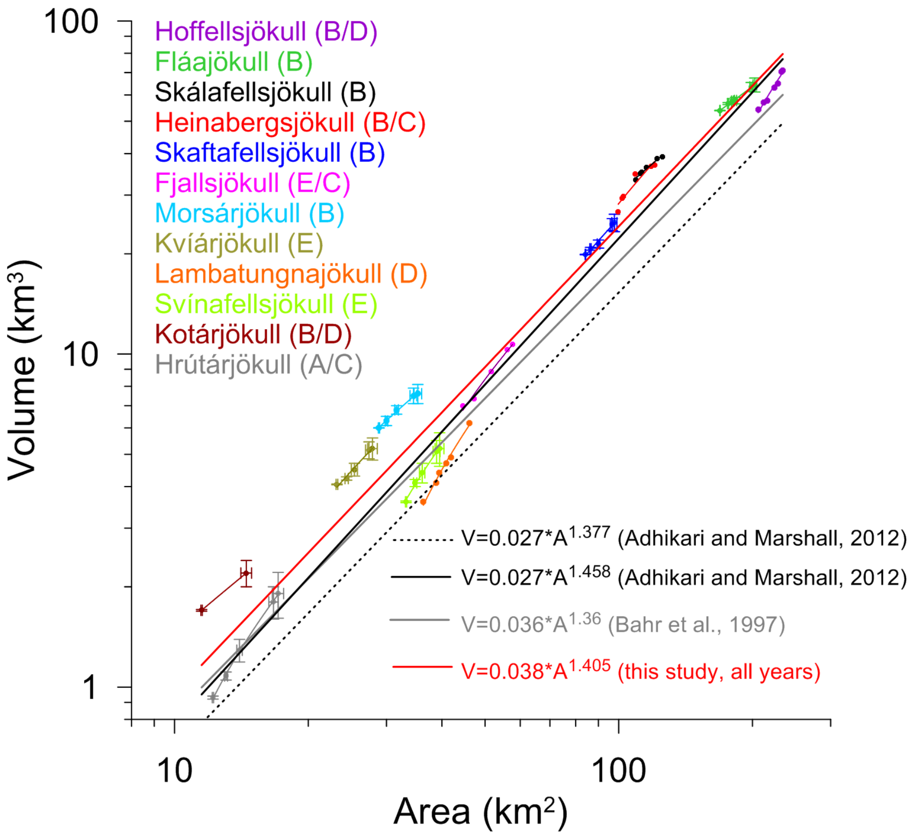

Figure 14. Volume-Area evolution of the individual outlet glaciers at ~ 1890, 1904, 1937, 1945, 1989, 2002, and 2010. The solid red line shows a least-squares fit to all the data points of this study, the solid gray line the corresponding least-squares line derived by Bahr (1997) for 144 glaciers, the solid black line the least-squares line dervied by Adhikari and Marshall (2012) for synthetic glaciers in steady state, and the dashed black line for the same glaciers after 100 years of retreat.